ANNUAL REVIEWS

Annual Review of Fluid Mechanics

Physicochemical Hydrodynamics of Particle Diffusiophoresis Driven by Chemical Gradients

Jesse T. Ault[1] and Sangwoo Shin[2]

[1]School of Engineering, Brown University, Providence, Rhode Island, USA

[2]Department of Mechanical and Aerospace Engineering, University at Buffalo, The State University of New York, Buffalo, New York, USA; email: sangwoos@buffalo.edu

Annu. Rev. Fluid Mech. 2025. 57:227–55

First published as a Review in Advance on September 25, 2024

The *Annual Review of Fluid Mechanics* is online at fluid.annualreviews.org

https://doi.org/10.1146/annurev-fluid-030424-110950

Keywords

diffusiophoresis, diffusioosmosis, colloids, chemical gradients, interfacial forces, physicochemical hydrodynamics

Abstract

Chemical gradients, the spatial variations in chemical concentrations and components, are omnipresent in environments ranging from biological and environmental systems to industrial processes. These thermodynamic forces often play a central role in driving transport processes taking place in such systems. This review focuses on diffusiophoresis, a phoretic transport phenomenon driven by chemical gradients. We begin by revisiting the fundamental physicochemical hydrodynamics governing the transport. Then we discuss diffusiophoresis arising in flow systems found in natural and artificial settings. By exploring various scenarios where chemical gradients are encountered and exploited, we aim to demonstrate the significance of diffusiophoresis and its state-of-the-art development in technological applications.

1. INTRODUCTION

Phoretic transport describes the directional migration of microscopic particulates driven by interfacial forces where both the migrating object and the surrounding fluid are force-free (Anderson 1989, Brady 2011). This process involves particles thermodynamically or mechanically interacting with the surrounding fluid, causing both the particles and the fluid in their vicinity to propel. To achieve phoretic transport, various driving forces can be harnessed from the surroundings [e.g., gradients of electric potential (electrophoresis), temperature (thermophoresis), or chemical potential (diffusiophoresis) (Anderson 1989)] or generated internally [e.g., metabolism (bacteria motility) (Ishikawa 2024)].

In this review, we discuss diffusiophoresis, a subtle yet universal phoretic transport mechanism for colloidal particles with broad implications in biological (Sear 2019, Ramm et al. 2021, Alessio & Gupta 2023, Doan et al. 2024), environmental (Möller et al. 2017), and industrial systems (Guha et al. 2015, Shin et al. 2018, Park et al. 2021). Historically, diffusiophoresis was first appreciated by Derjaguin and coworkers in the 1940s when they examined solvent osmosis and particle motion driven by the concentration gradients of neutral solutes (Derjaguin et al. 1947). Investigations with electrolytic solute gradients were undertaken in the early 1960s upon observing that the deposition rate of latex dipping of a glove was enhanced when the surface of the glove mold was precoated with $CaCl_2$ as a coagulant (Derjaguin et al. 1961). Their hypothesis, which has been recently brought into question (Williams et al. 2022, Groves et al. 2023), was that the concentration gradients of $CaCl_2$ established near the mold caused not only osmotic transport but also a diffusion-induced electric field strong enough to drive the migration of latex particles toward the surface of the mold, which resulted in a thicker coating. This led to the theoretical derivation of particle phoretic velocity induced by electrolyte gradients.

Then, in the 1980s and 1990s, Anderson, Prieve, and coworkers significantly advanced understanding of diffusiophoresis via analytical modeling (Anderson et al. 1982, Prieve et al. 1984, Anderson & Prieve 1991), numerical simulations (Prieve & Roman 1987), and experiments (Lin & Prieve 1983, Ebel et al. 1988). Since the advent of microfluidics and microfabrication in the 2000s, diffusiophoresis has elicited renewed interest in the fluids and soft matter communities (Velegol et al. 2016, Marbach & Bocquet 2019, Shin 2020, Shim 2022). Broadly speaking, research interests in diffusiophoresis have diverged into two directions: (*a*) exploiting diffusiophoresis as a means to achieve self-propelled microswimmers via chemical reactions in the context of active matter, where the chemical gradients are generated on the scale of the microswimmer's own body size, and (*b*) driving diffusiophoresis of passive colloidal particles via externally imposed chemical gradients in the background and utilizing the process in niche technological applications. While both directions share essentially the same phenomena and both can be described using exactly the same governing equations, the two research directions are often considered exclusive and discussed in different scientific communities. Lately, efforts have been put forth to provide a unified description that reconciles both directions of research (Ganguly et al. 2024).

This review is concerned with diffusiophoresis occurring on a passive particle driven by externally imposed solute concentration gradients. Readers interested in active diffusiophoresis (or self-diffusiophoresis) may refer to Moran & Posner (2017) and Bishop et al. (2023). This review begins by revisiting the governing transport physics of diffusiophoresis in Section 2. Then, in Section 3, we discuss colloidal diffusiophoresis in various background flows, such as shear, merging, and turbulent flows. In Section 4, we introduce some recent technological applications enabled by diffusiophoresis. Then we conclude this review in Section 5 by discussing several open questions.

2. PHYSICOCHEMICAL HYDRODYNAMICS OF DIFFUSIOPHORESIS

Diffusiophoresis is a multiscale interfacial phenomenon that is associated with the coupled transport of solutes, fluids, and colloidal particles occurring at various length scales. Solute and solvent molecules interact with the surface at the molecular scale (0.1 $\sim$ 10 nm). Perturbation of this interaction around the particle results in particle and fluid motion at the colloidal scale (0.01 $\sim$ 10 μm). At the meso-/macroscopic scale (>10 μm), the surrounding environment may affect the particle motion physically through geometrical confinements (Doan et al. 2021) or background flows (Ault et al. 2018) or chemically through surface reactions (Florea et al. 2014). The separation of such length scales makes it useful to approximate solute and solvent molecules as continua and treat their distribution and the interaction potential using a mean-field approach. In this review, we consider the diffusiophoretic phenomenon using a continuum description. This section begins by introducing solute–surface interactions at equilibrium, followed by an out-of-equilibrium scenario whereby introducing chemical gradients triggers fluid flow and particle motion. Readers interested in a molecular-level, micromechanical approach to the same problem may consult Brady (2011) and Ramírez-Hinestrosa et al. (2020).

2.1. Solute–Surface Equilibrium Interactions

The fundamental mechanism for the diffusiophoretic phenomenon lies in the nonequilibrium interactions between the surface and the neighboring solute. Consider an interaction potential $U(y)$ established near a flat surface, where y is the normal distance from the surface (**Figure 1*a***). The interaction force acting on the solute molecule due to this interaction potential is $-\mathrm{d}U/\mathrm{d}y$, and likewise, the force acting on the surface by that solute molecule is $\mathrm{d}U/\mathrm{d}y$. At thermodynamic equilibrium (i.e., in the absence of any chemical potential gradients), the solute distribution follows the Boltzmann relation $c(y) = c_\infty \exp[-U(y)/k_\mathrm{B}T]$, where c is the local solute concentration, k_B is the Boltzmann constant, T is the temperature, and c_∞ is the bulk solute concentration, which represents the concentration at a distance sufficiently far away from the surface such that the solute molecules are not influenced by the interaction potential. This distance, λ, corresponds to the range of the solute–particle interaction (e.g., the Debye screening length λ_D for Coulombic interactions), where the solute concentration differs substantially from the bulk concentration c_∞.

The interaction force acting on the solute molecules is transmitted to the neighboring solvent molecules, imparting an osmotic force on the fluid element, $\mathbf{f}_\mathrm{o} = \sum_i c_i(-\mathrm{d}U_i/\mathrm{d}y)\mathbf{j}$, and thus the osmotic pressure $\pi_\mathrm{o} = \int_0^\infty \mathbf{f}_\mathrm{o}\mathrm{d}y$ acting on the fluid by the interacting surface. The summation indicates that multiple solute species may contribute to the total osmotic force independently via various interactions.

The interaction potential $U(y)$ may take various forms depending on the nature of the solute–surface interactions. For instance, a charged surface can interact with ions predominantly through Coulombic interactions, whereas polar molecules can interact via charge–dipole interactions. Neutral species can interact via van der Waals or steric interactions. A list of expressions for some common interaction potentials between a solute molecule and a flat surface is provided in **Table 1** (Anderson 1989, Israelachvili 2011).

2.2. Flow via Nonequilibrium Solute–Surface Interactions: Diffusioosmosis

While the interaction force acts in the direction normal to the surface at equilibrium, it may vary along the surface when the system is perturbed, resulting in tangential stress at the interface. Let us consider an out-of-equilibrium system by introducing a concentration gradient of solute

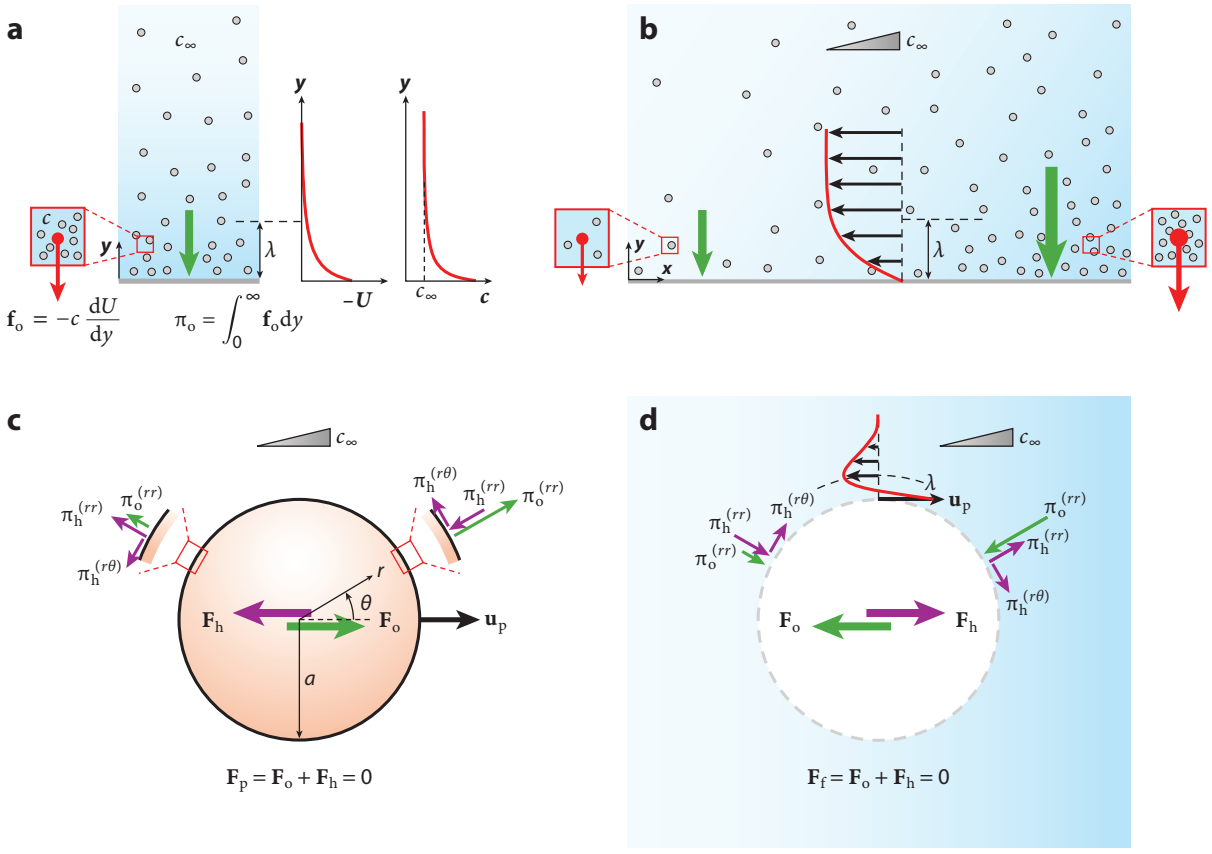

Figure 1

Motion of particles and fluids induced by concentration gradients of solute molecules interacting with the surface. (*a*) Solute distribution around an interacting surface at equilibrium. The (attractive) interaction potential U between the solute and the surface exerts volumetric force $\mathbf{f}_o$ on the fluid element that is proportional to the solute concentration, leading to the buildup of an osmotic pressure π_o within the interaction region of length λ. (*b*) When a solute concentration gradient is established tangent to the surface, the osmotic pressure is also varied along the surface, causing fluid flow (diffusioosmosis). (*c*,*d*) When a solute concentration gradient is established around a freely suspended sphere, the osmotic interaction force acted by the fluid pulls the particle toward the higher concentration side at a velocity $\mathbf{u}_p$ (diffusiophoresis) while the same but opposite force pushes the adjacent fluid to the back by diffusioosmosis. In such cases, both the particle and the fluid are force-free; panel *c* illustrates the forces acting on the particle by the fluid, whereas panel *d* depicts the forces acting on the adjacent fluid by the particle.

molecules along the surface in the far field ∇c_∞ (**Figure 1*b***). In this scenario, the osmotic force acting on the fluid element $\mathbf{f}_o$, and hence the fluid osmotic pressure π_o, must vary tangentially along the surface since they are dependent on the local solute concentration. This pressure imbalance will cause fluid elements within the interfacial region to accelerate until they are balanced by the viscous stress. Such osmotically driven fluid flow is referred to as diffusioosmosis, which can be described by solving the Stokes equations

$$\nabla \cdot \mathbf{u}_f = 0, \quad \mathbf{0} = -\nabla p + \eta \nabla^2 \mathbf{u}_f + \mathbf{f}_o, \qquad 1.$$

where $\mathbf{u}_f$ is the fluid velocity, p is the pressure, η is the fluid viscosity, and $\mathbf{f}_o = -\sum_i c_i \nabla U_i$ is the osmotic interaction force felt by the unit fluid volume containing solute species i of concentration c_i. The steady-state solute flux $\mathbf{j}_i$ and the distribution c_i, which are also influenced by the interaction

Table 1 Some common expressions for interaction potential $U(y)$ between a solute molecule and a flat surface

Interaction	Potential[a]	Note(s)
Coulombic	$U(y) = ze\zeta e^{-y/\lambda_D}$	Low potential[b] (Debye–Hückel)
	$U(y) = 2k_BT \ln\left(\frac{1+\gamma e^{y/\lambda_D}}{1-\gamma e^{y/\lambda_D}}\right)$	z:z electrolyte (Gouy–Chapman)
Dipolar	$U(y) = k_BT\left\{1 - \frac{4\mu}{ze\lambda_D} \cdot \frac{\gamma e^{-y/\lambda_D}}{1-\gamma^2 e^{-2y/\lambda_D}} \cdot \coth\left(\frac{4\mu}{ze\lambda_D} \cdot \frac{\gamma e^{-y/\lambda_D}}{1-\gamma^2 e^{-2y/\lambda_D}}\right)\right\}$	z:z supporting electrolyte
Steric	$U(y) = \left(\frac{R}{y}\right)^n$	$n \to \infty$ for hard repulsion
		$n \approx 9$–16 for soft repulsion
Van der Waals	$U(y) = -\frac{\pi C\rho}{6y^3}$	

[a]Here z is the charge number; e the elementary charge; $\lambda_D = \sqrt{\frac{\epsilon k_BT}{e^2\sum_i c_i z_i^2}}$ the Debye screening length; ϵ the permittivity of the solution; ζ the zeta potential; $\gamma = \tanh\left(\frac{ze\zeta}{4k_BT}\right)$; μ the solute dipole moment; R the solute radius; C the coefficient in the atom-atom pair potential; and ρ the molecular number density of the wall.
[b]$\zeta < \frac{k_BT}{ze}$.

force, can be described by the Smoluchowski advection–diffusion equations

$$\nabla \cdot \mathbf{j}_i = 0, \quad \mathbf{j}_i = -D_i\nabla c_i + c_i\mathbf{u}_f - \frac{D_ic_i}{k_BT}\nabla U_i, \qquad 2.$$

where D_i is the diffusivity of solute species i.

When the solute is charged (an ion, polyelectrolyte, ionic liquid, etc.), fluid flow over a charged wall is driven not only by osmotic stress but also by electric (Maxwell) stress. The local electroneutrality of the solute species enforces zero ionic current ($\sum_i z_i e\mathbf{j}_i = 0$), causing an electric field to arise in the far field. Neglecting advective transport, the electric field reads (Chiang & Velegol 2014, Gupta et al. 2019)

$$\mathbf{E} = \frac{k_BT}{e}\frac{\sum_i z_iD_i\nabla c_{i,\infty}}{\sum_i z_i^2D_ic_{i,\infty}}. \qquad 3.$$

For a symmetric binary (z:z) electrolyte, this electric field simply reduces to $\mathbf{E}_{z:z} = \frac{k_BT}{ze}\beta\nabla\ln c_\infty$, where $\beta = \frac{D_+-D_-}{D_++D_-}$ is the dimensionless diffusivity contrast between the cation (+) and the anion (–). This electric field induced by the asymmetric diffusion of ionic solutes drives the electroosmotic flow. Therefore, solute gradients can induce diffusioosmosis via two independent driving forces: osmotic stress and electric stress. It is common in the literature to explicitly distinguish the osmotic contribution from the electric contribution by referring to the osmotically driven flow as chemiosmosis, so that diffusioosmosis encompasses chemiosmosis and electroosmosis when the solute is charged.

2.3. Motion of Freely Suspended Surfaces: Diffusiophoresis

When the surface is freely suspended, as in the case of colloidal particles, the spatial imbalance in the surface stress will cause the surface to move. Consider a rigid, spherical particle with a radius of a immersed in an unbounded fluid containing solute molecules that interact with the particle surface through the same interaction potential U (**Figure 1*c***). In this scenario, the osmotic force felt by the particle $\mathbf{F}_o$ is stronger at the side of higher solute concentration compared to the lower-concentration side, resulting in particle motion toward higher solute concentration at the particle velocity $\mathbf{u}_p$ at steady state. In essence, the particle is being pulled by the attractively interacting solute molecules. Simultaneously, the same osmotic force felt by the adjacent fluid drives diffusioosmosis in the opposite direction (**Figure 1*d***).

Table 2 Some analytical solutions for the diffusiophoretic velocities in the limit of vanishingly thin interfacial layer ($a/\lambda \to \infty$)

Solute	Particle velocity	Key assumption(s)	Reference(s)
Ionic	$\mathbf{u}_p = \frac{\epsilon}{\eta}\left(\frac{k_B T}{ze}\right)^2 \left\{\beta \frac{ze\zeta}{k_B T} + 4\ln\cosh\left(\frac{ze\zeta}{k_B T}\right)\right\} \nabla \ln c_\infty$	$z{:}z$ electrolyte	Derjaguin et al. 1961, Prieve et al. 1984
	$\mathbf{u}_p = \frac{\epsilon}{\eta}\left(\frac{\sum_i z_i^2 \nabla c_{i,\infty}}{\sum_i z_i^2 c_{i,\infty}} \frac{\zeta^2}{8} + \frac{k_B T}{e} \frac{\sum_i z_i D_i \nabla c_{i,\infty}}{\sum_i z_i^2 D_i c_{i,\infty}} \zeta\right)$	Small zeta potential	Chiang & Velegol 2014, Gupta et al. 2019
Polar	$\mathbf{u}_p = \frac{k_B T}{3\eta}\left(\frac{2\mu\gamma}{ze}\right)^2 \left[1 + \frac{\gamma^2}{2}\left\{1 + \frac{4}{5}\left(\frac{\mu}{ze\lambda_D}\right)^2\right\}\right] \nabla c_\infty$	$z{:}z$ supporting electrolyte	Anderson 1989
Neutral	$\mathbf{u}_p = -\frac{k_B T}{2\eta} R^2 \nabla c_\infty$	Hard sphere	Anderson 1989, Staffeld & Quinn 1989

The forces acting on the particle by the surrounding fluid are the hydrodynamic force $\mathbf{F}_h$ due to diffusioosmosis and Stokes drag and the osmotic force $\mathbf{F}_o$ due to the particle–solute interactions. At steady state, the total force acting on the particle $\mathbf{F}_p$ must vanish:

$$\mathbf{F}_p = \mathbf{F}_o + \mathbf{F}_h = \int_A \mathbf{n} \cdot (\pi_o + \pi_h) dA = \mathbf{0}, \quad 4.$$

where $\mathbf{n}$ is the normal unit vector pointing outward from the particle surface A. π_h and π_o are the hydrodynamic and osmotic stresses acting on the particle surface, respectively. Solving this equation allows one to find the diffusiophoretic velocity of the particle $\mathbf{u}_p$; some known analytical solutions in the limit of the vanishing interfacial layer ($a/\lambda \to \infty$) are provided in **Table 2**.

For electrolytic diffusiophoresis, it is a common practice to write the velocity as $\mathbf{u}_p = \mathcal{M} \nabla \ln c_\infty$, where $\mathcal{M}$ is the diffusiophoretic mobility, which quantifies the strength of diffusiophoretic motion for a given solute gradient (Prieve et al. 1984). For symmetric electrolytes in the limit of zero Debye length, the mobility reads

$$\mathcal{M} = \frac{\epsilon}{\eta}\left(\frac{k_B T}{ze}\right)^2 \left\{\beta \frac{ze\zeta}{k_B T} + 4\ln\cosh\left(\frac{ze\zeta}{k_B T}\right)\right\}, \quad 5.$$

where ϵ is the permittivity of the solution. The first and the second terms on the right-hand side represent contributions from electric (electrophoresis) and osmotic (chemiphoresis) forces, respectively. This expression was originally established by Derjaguin and coworkers (Derjaguin et al. 1961) and then later formally derived by Prieve, Anderson, and coworkers (Prieve et al. 1984). While this description assumes that the mobility is independent of the local solute concentration, it is not necessarily true as the surface charge is often heavily influenced by the local chemistry of the solution. Because the particles being transported in diffusiophoretic systems experience transient, spatially varying solute concentrations, it is critical to use a correct model for the diffusiophoretic mobility that accounts for variable zeta potential effects (see, e.g., Kirby & Hasselbrink 2004, Akdeniz et al. 2023, Lee et al. 2023).

The availability of the analytical solutions for the particle velocity $\mathbf{u}_p$ and the flow field $\mathbf{u}_f$ has been largely based on how the interfacial layer is treated. Typically, the limiting case is when the interfacial layer is vanishingly thin compared to the scale of the particle (e.g., **Table 2**). This scale mismatch allows any details within the interfacial region to be lumped into an effective slip flow, where the relative velocity between the fluid at the edge of the interfacial layer [$\mathbf{u}_f(r = a + \lambda) = \mathbf{u}_f^\lambda$] and at the particle surface [$\mathbf{u}_f(r = a) = \mathbf{u}_p$] can be considered as a slip velocity on the particle surface, $\mathbf{u}_{slip} = \mathbf{u}_f^\lambda - \mathbf{u}_p$. Then, based on Lamb's solution of the Stokes equations with zero net force acting on the surface that encloses both the particle and the interfacial layer, the particle velocity can be expressed as $\mathbf{u}_p = -\langle \mathbf{u}_{slip} \rangle$, where $\langle \cdot \rangle$ is the area average over the particle surface.

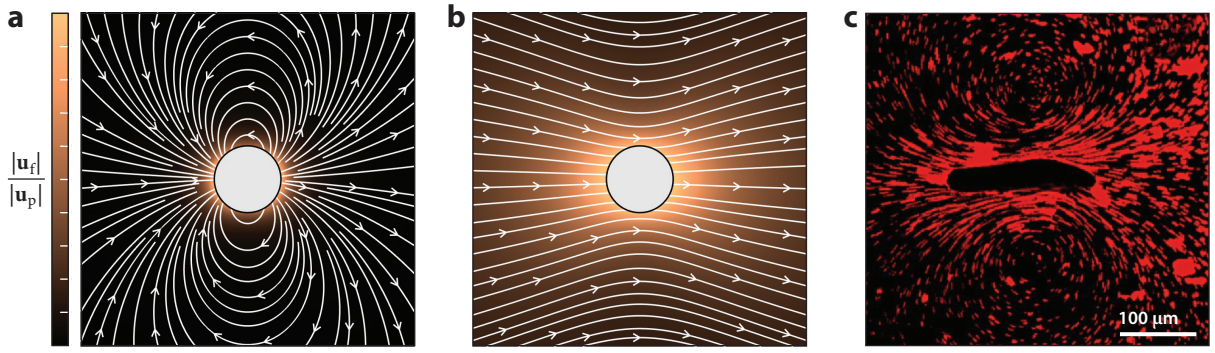

Figure 2

Fluid flow around a moving particle. (*a*,*b*) Flow fields around particles moving to the right-hand side with a velocity magnitude of $|\mathbf{u}_p|$ in the lab reference frame driven by (*a*) diffusiophoresis and (*b*) sedimentation. $|\mathbf{u}_f|$ is the flow velocity magnitude. (*c*) Flow field around *Paramecium*. Panel *c* adapted with permission from Jana et al. (2012).

This also allows the fluid flow outside the interfacial region to be described by a potential flow (Anderson 1989).

Another common assumption is to neglect advective transport in the interfacial layer so that the interfacial structure does not polarize and remains spherical. As the fluid flow disrupts the solute distribution, the interfacial layer is polarized, which effectively weakens the driving force, thus reducing the particle velocity (Prieve & Roman 1987). Dismissing this effect requires the solute Péclet number $\mathrm{Pe}_s = u_p a/D$ to be much smaller than unity, which allows the decoupling of fluid flow (Equation 1) and solute transport (Equation 2).

The force-free condition (Equation 4) also has a profound influence on the fluid flow around the particle. As the net force acting on the bulk fluid $\mathbf{F}_f$ is also zero (**Figure 1*d***), the flow around the particle outside the interfacial region is significantly less perturbed, which is one of the key features of phoretic transport (Anderson 1989). The resulting external flow field outside the interfacial region can be described by a source dipolar flow (**Figure 2*a***):

$$\mathbf{u}_f(\mathbf{x}) = \frac{1}{2}\left(\frac{a}{r}\right)^3 \left(3\frac{\mathbf{xx}}{r^2} - \mathbf{I}\right) \cdot \mathbf{u}_p, \qquad 6.$$

where $\mathbf{x}$ is the position vector and $\mathbf{I}$ is the identity matrix. This flow field is in stark contrast to that created by a particle dragged via external force, e.g., gravity for a sedimenting sphere, which is effectively described by a force monopolar flow (**Figure 2*b***).

We note that the flow field around a diffusiophoretic particle has a close resemblance to the flow around motile microorganisms despite the origin of the propulsive force being different (Ishikawa 2024). For instance, *Paramecium*, which is a eukaryotic ciliate, generates fluid flow via asymmetric beating of microscopic cilia covering the cell body. This action produces interfacial flow over the body surface, akin to diffusioosmosis (**Figure 2*c***). In this regard, (self-)diffusiophoretic particles are often utilized to emulate the active motion of motile microorganisms (Moran & Posner 2017).

While the total force acting on the diffusiophoretic particle is zero, the local stress acting on the particle surface $\pi(\theta) = \pi_h + \pi_o$ does not necessarily vanish, as recently identified by Marbach et al. (2020). They calculated the force distribution on a rigid sphere in the limits of zero Pe_s and discussed that the nonzero local stress distributed over the particle surface by diffusiophoresis may deform soft particles, such as vesicles and droplets.

In the case of a viscous Newtonian drop, McKenzie et al. (2022) showed that a linear solute gradient, which is commonly employed in microfluidic experiments (Palacci et al. 2010, Paustian

et al. 2013, Shi et al. 2016, Rasmussen et al. 2020), is insufficient to induce deformation as the stress acting on the exterior drop surface is balanced out by the hydrodynamic stress acting on the interior surface of the drop. Thus, the authors suggested that higher-order gradients are required to induce any appreciable deformation of viscous drops via diffusiophoresis. Nonetheless, how the rheology (bulk and interfacial viscoelasticity) affects the deformation of non-Newtonian drops (e.g., gels, vesicles, coacervates, and surfactant-laden drops) by diffusiophoresis remains an open question.

2.4. Curvature Effect: Size and Shape Dependence

The curvature of a particle's surface has an influence on the diffusiophoretic velocity if the thin interfacial layer approximation is relaxed. Physically, a convex curvature effectively reduces the solute distribution near the curved surface of a particle compared to a flat surface. The osmotic driving force is thus weakened, leading to a slower migration velocity (Anderson et al. 1982). Similar to the Henry function for electrophoresis, analytical solutions to the size-dependent factors for diffusiophoresis were developed for $z{:}z$ electrolytes (Prieve et al. 1984, Keh & Wei 2000), which were also verified experimentally (Ebel et al. 1988, Shin et al. 2016).

In a similar manner, the curvature effect can lead to shape-dependent diffusiophoresis, implying the migration may also be sensitive to the orientation of the particle relative to the imposed solute gradient. Earlier theoretical studies predicted that the particle curvature relevant to the migration direction dominates the particle motion (Dukhin 1993). For instance, a cylinder or a prolate spheroid migrating along its major principal axis will experience migration similar to the flat surface, whereas migrating along the minor axis will be close to the sphere of the same radius. This was recently validated by Doan et al. (2023) experimentally, where the migration velocity and the particle's orientation angle were observed to be strongly correlated (**Figure 3*a*,*b***). Taking the radius of curvature along the direction of the solute gradient as an effective radius of a sphere, they showed that this sphere approximation effectively captures the shape- and orientation-dependent diffusiophoresis of colloidal ellipsoids.

2.5. Boundary Confinement Effect

When a particle is near a wall, hydrodynamic effects increasingly restrict the particle's motion as the separation between the particle and the wall decreases (Happel & Brenner 1983). Particles undergoing diffusiophoresis near boundaries also experience similar effects, but due to the driving forces also affected by the boundaries, particles may exhibit nonintuitive behavior. In particular, near-wall hydrodynamic interactions alter the diffusive and convective transport of the solutes, and interactions between the wall and the interfacial layers may not only decrease the particle motion, but rather enhance or even reverse the direction of diffusiophoresis. Theoretical progress toward understanding these coupled dynamics near fixed walls has been primarily focused on three scenarios: (*a*) particles near planar walls, (*b*) particles inside circular tubes or spherical cavities, and (*c*) particles inside porous media.

The original work on the boundary effects on diffusiophoresis dates back a few decades, where Keh, Anderson, and Chen investigated electrophoresis of a charged sphere moving parallel or perpendicular to a flat surface in the limit of a vanishingly thin Debye layer ($a/\lambda_D \to \infty$) (Keh & Anderson 1985, Keh & Chen 1988). In such a limit, the dipolar flow fields around the particle undergoing electrophoresis and diffusiophoresis are identical so that diffusiophoresis near a boundary can be interpreted from electrophoresis results. While the influence of boundaries on diffusiophoretic particles is generally weaker compared to sedimenting particles due to the reduced hydrodynamic interactions (cf. **Figure 2*a*,*b***), Keh, Anderson, and Chen showed that

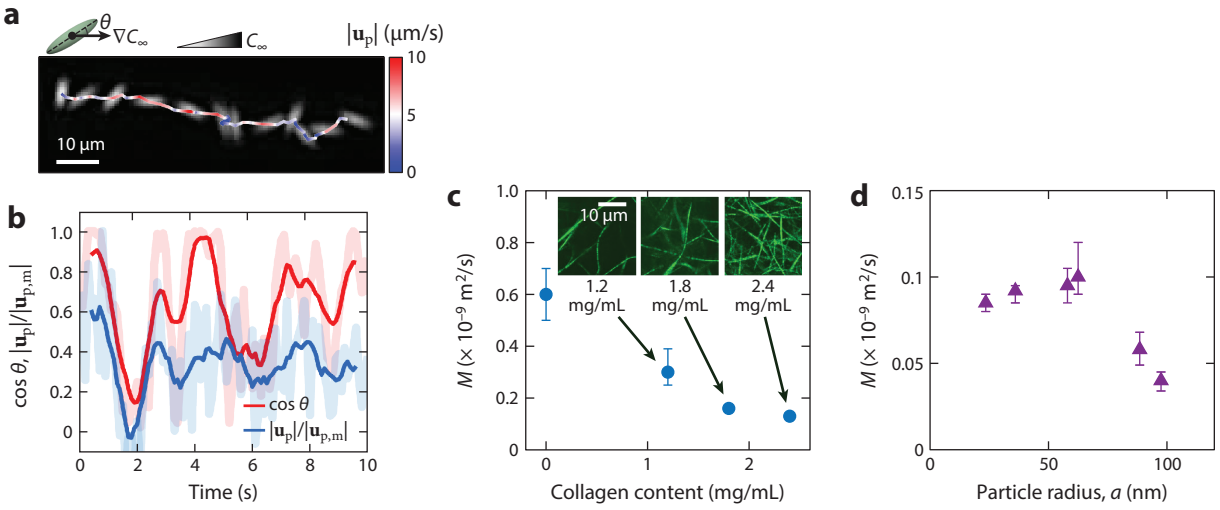

Figure 3

Factors affecting particle diffusiophoresis. (*a*,*b*) Orientation-dependent diffusiophoresis of colloidal ellipsoids. (*a*) A time-lapse image (10-s interval between successive images) of a charged ellipsoid (aspect ratio of 6.5) undergoing diffusiophoresis via salt gradients. The particle trajectory is overlaid on the image. Color represents the velocity magnitude. (*b*) A plot of particle velocity magnitude $|\mathbf{u}_p|$ normalized by the maximum velocity magnitude $|\mathbf{u}_{p,m}|$ and $\cos\theta$, where θ is the angle between the ellipsoid's major axis and the chemical gradient in the far field. (*c*,*d*) Confinement-dependent diffusiophoresis of spherical nanoparticles in a collagen matrix. Shown are the diffusiophoretic mobility of (*c*) amine-functionalized nanoparticles (radius of 100 nm) at varying collagen concentrations and (*d*) polystyrene-*b*-polyethylene glycol nanoparticles of varying radius at a fixed collagen concentration of 2.4 mg/mL. Insets in panel *c* are confocal images of the collagen matrix at different concentrations. Panels *a* and *b* adapted with permission from Doan et al. (2023). Panels *c* and *d* adapted with permission from Doan et al. (2021).

with increasing confinement the diffusiophoretic driving force (i.e., solute gradients) strengthens at the gap and leads to faster migration at extremely tight confinement compared to the free space migration despite increased viscous drag from the wall. However, once the thin Debye layer approximation is relaxed such that the details of the Debye layer are taken into consideration, diffusiophoresis and electrophoresis are no longer identical due to their difference in the transport processes within the Debye layer.

Since then, numerous efforts have been put forth by Keh and others to understand the boundary confinement effects on diffusiophoresis of spherical and cylindrical particles near planar or curved boundaries at finite Debye lengths, where the Debye layer around a particle may polarize (Keh 2016). In this scenario, the Debye layer may further deform by interacting with a charged wall. With the compression of the Debye layer, nonlinear effects can arise that lead to complex particle behaviors that are not straightforward to predict, where the particle velocity no longer changes monotonically with the particle surface charge, Debye length, or gap spacing (Lee et al. 2010, Chiu & Keh 2017).

For nonspherical particles such as cylinders and spheroids, the boundary effects are generally expected to be stronger than for spherical particles due to the enlarged particle–wall interaction area. Boundary effects for cylindrical particles were also found to either increase or decrease the particle diffusiophoresis or even reverse its direction (Joo et al. 2010, Hsu et al. 2012).

Extending the results near simple surfaces to general porous media flows is not trivial, and in fact, several studies specifically emphasized the nongeneralizability of the results due to strong geometry dependence (Chen & Keh 2005, Chang & Keh 2008). That being said, additional studies have sought to understand diffusiophoresis in several specific geometries relevant to porous media.

The first class of these studies involves particle transport through a fibrous medium consisting of a regular array of cylindrical obstacles. The purely electrophoretic migration in such a fiber matrix was solved theoretically using a unit cell model (Kozak & Davis 1986, E. Lee et al. 2000), which was further extended to diffusiophoresis at arbitrarily oriented solute gradients and arbitrary Debye lengths (Keh & Hsu 2008, 2009).

Experimentally, diffusiophoresis of nanoparticles in collagen hydrogels was studied by Doan et al. (2021), where collagen is a fibrous biopolymer that forms into a random fibrous matrix when crosslinked (Antoine et al. 2014). The particle motion was shown to be either monotonic or nonmonotonic with respect to the degree of confinement, depending on how the confinement is varied. For instance, it was shown that the mobility of a particle with a constant radius generally decreases with decreasing pore size (increasing gel concentration; **Figure 3*c***), whereas the mobility exhibits a nonmonotonic trend when the particle size is varied while keeping the pore size the same (**Figure 3*d***). This nonmonotonic mobility is due to the competing effects of curvature and confinement. Doan et al. (2021) applied the unit cell model for electrophoresis developed by Zydney (1995) and combined it with the steric factor of the fibrous matrix (Johansson & Löfroth 1993) to capture the nonmonotonic diffusiophoresis in collagen hydrogels. Further theoretical investigations were conducted by Bhaskar & Bhattacharyya (2023) and Sambamoorthy & Chu (2023) using the Brinkman approximation for solvent transport, which effectively captured the experimental observations shown in **Figure 3*c,d***.

3. DIFFUSIOPHORESIS IN BACKGROUND FLOWS

In this section, we discuss the emergent colloid dynamics that arises when particles experience diffusiophoresis in the presence of background flows. While diffusiophoresis could be considered in virtually any flow problem, there are several key systems and configurations that are commonly encountered in microfluidic as well as other industrial and natural systems. The three types of typical systems that we consider are (*a*) diffusiophoresis in unidirectional shear flows (**Figure 4*a***), in which the coupling can result in features such as enhanced or arrested particle dispersion, rectified motion, focusing, and separation; (*b*) diffusiophoresis in merging flows (**Figure 4*b***), in which the coupling of solute gradients at a flow junction can lead to particle trapping, transverse spiraling, and particle separations; and (*c*) diffusiophoresis in vortical or turbulent flows (**Figure 4*c***), in which the particle diffusiophoresis may be promoted by enhanced chemical dispersion.

3.1. Boundary Layer Interactions

Solute transport subject to a shear flow near a bounded wall results in the formation of solute boundary layers, creating solute gradients perpendicular to the wall. Subsequent particle diffusiophoresis can cause cross-stream segregation of colloidal particles when the solute is continuously

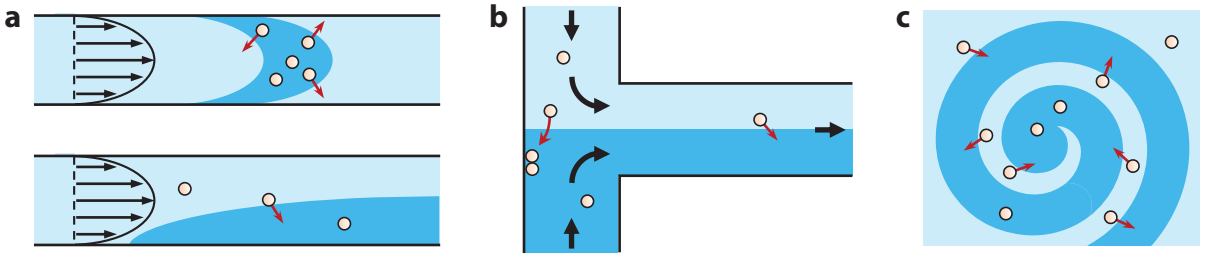

Figure 4

Possible scenarios of particle diffusiophoresis in (*a*) Poiseuille, (*b*) merging, and (*c*) vortical flows in the background.

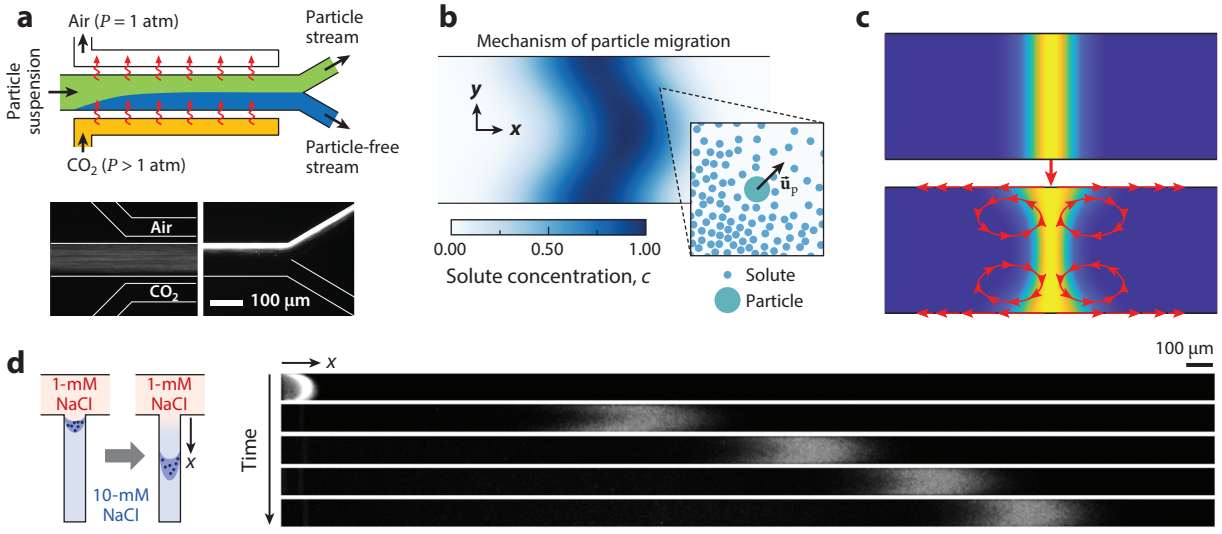

Figure 5

Particle dispersion via diffusiophoresis in shear flows. (*a*) Cross-stream diffusiophoresis in a straight channel enabled by the dissolution of CO_2 gas. (*b*) Dispersion-enhanced particle diffusiophoresis in a background Poiseuille flow. (*c*) Diffusioosmosis-driven dispersion in an initially quiescent channel flow. The color schemes in panels *b* and *c* represent solute concentrations. (*d*) Dispersion of a patch of colloidal particles in a dead-end pore by diffusiophoresis and diffusioosmosis. Panel *a* adapted from Shin et al. (2017c) (CC BY 4.0). Panel *b* adapted with permission from Migacz & Ault (2022). Panel *c* adapted with permission from Teng et al. (2023). Panel *d* adapted from Alessio et al. (2022) (CC BY 4.0).

released near the wall (**Figure 5*a***). When a finite patch of solute is introduced, diffusiophoresis could lead to enhanced or arrested particle dispersion through Taylor-dispersion-like behavior (**Figure 5*b***).

3.1.1. Cross-stream diffusiophoresis in straight channel flows. One of the simplest systems in which the coupled fluid, solute, and particle dynamics can be investigated is in the shear flow next to a reacting wall in a long, straight channel. Techniques ranging from the use of gas-permeable membranes to allow the exchange of soluble, dissociable gases (Shin et al. 2017c) to porous media (K. Lee et al. 2020) to ion-exchange membranes (Florea et al. 2014, Lee et al. 2018) for direct exchange of solute can be incorporated into a microfluidic device to generate a source or sink of ions at the channel walls. Coupled with a background pressure-driven fluid flow, the ions diffuse perpendicular to the flow, creating a solute boundary layer that leads to particle exclusion or focusing near the wall via diffusiophoresis.

For instance, one system that has found recent use is a simple system consisting of three parallel channels separated by thin polydimethylsiloxane (PDMS) walls (Shin et al. 2017c) (**Figure 5*a***). Suppose the center channel flows a solution containing colloidal particles and the two side channels flow CO_2 gas and air, respectively. Due to the gas permeability of the PDMS walls (Merkel et al. 2000), some CO_2 will permeate through the side wall, where it will dissolve into the solution in the center channel and partially dissociate into H^+ and HCO_3^- ions. The combined diffusion/advection of these ions from the wall then sets up a cross-flow ion gradient in the main channel that can drive cross-stream migration of the suspended particles. The dynamics of this coupled transport is determined by the particle Péclet number, $\mathrm{Pe_p} = \frac{\overline{u}_f w^2}{|\mathcal{M}|l}$, which compares the relative timescales of convection along the length l of the flow ($\overline{u}_f/l$, where $\overline{u}_f$ is the mean flow speed) to particle diffusiophoresis across the width w of the channel ($|\mathcal{M}|/w^2$) (Shimokusu et al.

2020). As such, the cross-stream migration of particles depends on particle mobility, so that particles of different sizes or surface charge can be expected to migrate at different rates, enabling applications such as filtration and separation (Shin 2020). As mentioned, a variety of alternative options to create a source or sink of ions at the channel walls exist, but in any case, the ion concentration is governed by similar dynamics, as well as the growth of the particle exclusion/focusing zone. In the limit of long, narrow channels at relatively high Pe_p, the leading-order particle velocity is simply $\mathbf{u}_\mathrm{p} = u_\mathrm{f}(y,z)\mathbf{i} + \mathcal{M}\frac{\mathrm{d}\ln c}{\mathrm{d}y}\mathbf{j}$, where $u_\mathrm{f}(y,z)$ is the pressure-driven velocity profile in the channel (flow direction assumed to be $+x$), and $\frac{\mathrm{d}\ln c}{\mathrm{d}y}$ is the gradient of the ion concentration normal to the flow direction. This simple leading-order dynamics facilitates straightforward calculation for flow-based separation systems.

3.1.2. Diffusiophoretic dispersion. In the presence of a background shear flow, dispersion plays a critical role in the coupled particle/solute dynamics for systems involving diffusiophoresis (Chu et al. 2021, 2022; Migacz & Ault 2022). As a simple illustration of this point, consider a pressure-driven pipe flow where a patch of concentrated solutes and colloidal particles is suddenly introduced. At timescales much longer than the diffusion timescales of both solute and particles across the channel diameter, the dynamics will be approximately one-dimensional (1D), with both concentration fields being advected along at the mean flow speed, and as the solute diffuses and advects along the length of the pipe, the particles will be attracted or repelled from the solute peak. At earlier time regimes, the solute and particle fields can both experience Taylor-dispersion-like effects, via the shear flow distorting the patches of solute and particles from their 1D profiles. In the absence of diffusiophoresis, both solute and particle concentrations would experience typical Taylor dispersion, in which an initial profile that is uniform over the cross section is distorted by the relatively faster flow along the channel center, resulting in a distorted diffusing patch of concentrations (Taylor 1953). However, when the particle field also experiences diffusiophoresis, the cross-flow solute concentration gradients due to the distorted solute field drive particle motion toward or away from the channel walls (**Figure 5*b***). Although the variation in solute concentration across the channel may be small in the long, narrow channels in which these effects are typically considered, because it acts over a relatively shorter length scale, the cross-stream diffusiophoresis can be the same order of magnitude as the diffusiophoresis along the flow that is the dominant behavior in the 1D limit (Migacz & Ault 2022).

Whether and how diffusioosmosis on the channel wall may alter this coupled behavior depend on the relative balance of the diffusioosmotic flow on the channel walls, the diffusiophoresis of the particles, and the mean flow speed. As a simple illustration, consider a similar channel flow where a patch of solute and particles is introduced in the absence of background pressure-driven flow (**Figure 5*c***). If diffusioosmosis acts on the system, it will drive a slip flow at the walls toward or away from the solute concentration peak depending on the sign of the mobility. In turn, a pressure-driven flow will build up in the opposite direction along the channel centerline to conserve mass. Thus, four transient, recirculating flow cells will develop in the system, and these shear flows will in turn distort the solute profile as it diffuses by Taylor-dispersion-like effects (Teng et al. 2023).

3.1.3. Flows in dead-end pores. One of the widely used geometries for studying diffusiophoresis in microfluidics devices is the dead-end pore system, due to the simple geometry that allows easy experiments (Kar et al. 2015, Shin et al. 2016, Shi & Abdel-Fattah 2021, Tan et al. 2021) and calculations (Ault et al. 2017, Alessio et al. 2022). This system's relatively confined nature makes it a convenient analog for studies in more complicated systems such as porous media, hydraulic fractures, and other confined biological or geological systems. The typical approach to introduce a solute gradient into a dead-end pore is to flow a solution containing one solute concentration past the entrance of the pore containing a different solution, which drives diffusion between the two

solutions (Shin et al. 2016). The resulting transient solute gradient can drive the particles into or out of the pore via diffusiophoresis. Such transient solute gradients can also drive diffusioosmosis and recirculating flows in the pore. In fact, these diffusioosmosis-driven flows can be sufficient to transport particles into or out of the pores even in the absence of diffusiophoresis (Kar et al. 2015, Shin et al. 2016).

As hinted in the previous section, diffusiophoretic/diffusioosmotic transport in dead-end pores typically falls into the category of dispersion processes described above (**Figure 5*d***). That is, while the diffusioosmotic recirculating flows in these systems certainly drive dispersion of the solute and particle fields, also yielding the cross-stream diffusiophoresis that may result in significant focusing, nonetheless the concentration deviations over the cross section tend to be small, such that simplified macrotransport equations are often sufficient to effectively capture the nearly 1D dynamics (Alessio et al. 2022). These can be used in conjunction with the theoretical solutions for the leading-order solute/particle dynamics in a dead-end pore, including the propagating particle front dynamics, which have previously been derived in the limit of a long, narrow pore using a similarity analysis and the method of characteristics (Ault et al. 2017). One intriguing result of extending these analyses to higher order is that the average motion of the particles in the pore is primarily determined by diffusiophoresis, whereas the dispersion of the particle concentration field is governed by diffusioosmosis (Alessio et al. 2022).

Due to the simplicity of establishing controlled, predictable solute gradients with relatively confined background flow, the dead-end pore system serves as a valuable platform for many types of diffusiophoretic studies, and these systems have been used, for example, to measure particle zeta potential and diffusiophoretic mobility (Shin et al. 2017a, Akdeniz et al. 2023), to characterize the influence of solute type (Wilson et al. 2020, Shim et al. 2022, Akdeniz et al. 2024), and to test various models for mobility relations (Gupta et al. 2020b, Lee et al. 2023). Finally, while the role of diffusiophoresis has typically been considered inside the dead-end pore, the propagation of the solute gradients out of the pore entrance into the bulk flow suggests that diffusiophoresis outside of the pore also plays a role in particle capture and ejection from the pores. For example, when multiple pores are arranged in parallel, particles flowing past the pore entrances exhibit drift further toward the entrances with each subsequent hop past a pore, highlighting the pore-scale diffusiophoretic mechanism that ultimately leads to particle capture (Battat et al. 2019), which also has implications in anomalous particle dispersion in porous media (Jotkar et al. 2024).

3.2. Merging Flows

Another straightforward approach to generate solute gradients is through the direct mixing of two or more flow streams of different solute concentrations. Through judicious choice of flow configuration, mixing solute streams can be used to establish solute gradients both normal and parallel to the flow direction. For example, coflowing of different solute streams in Ψ-shaped channels can be used to establish long-duration cross-flow solute gradients downstream (**Figure 6*a*,*b***), whereas merging flows at T-junctions can be used to establish sharp local solute gradients in the vicinity of the junction (**Figure 6*c*,*d***).

3.2.1. Ψ-shaped merging flows. Ψ-shaped channels represent simple flow systems for performing diffusiophoretic experiments because of their ubiquity in microfluidics and for the ease of mixing flow streams to establish cross-stream solute gradients. In these systems, steady-state solute gradients can be easily established, and the diffusiophoretic transport typically occurs normal to the primary flow direction. The canonical example of this flow system is with three inlets merging symmetrically into a long, straight flow channel (Abécassis et al. 2008) (**Figure 6*a***). The critical decisions for this system are which inlets will contain solute and which will contain

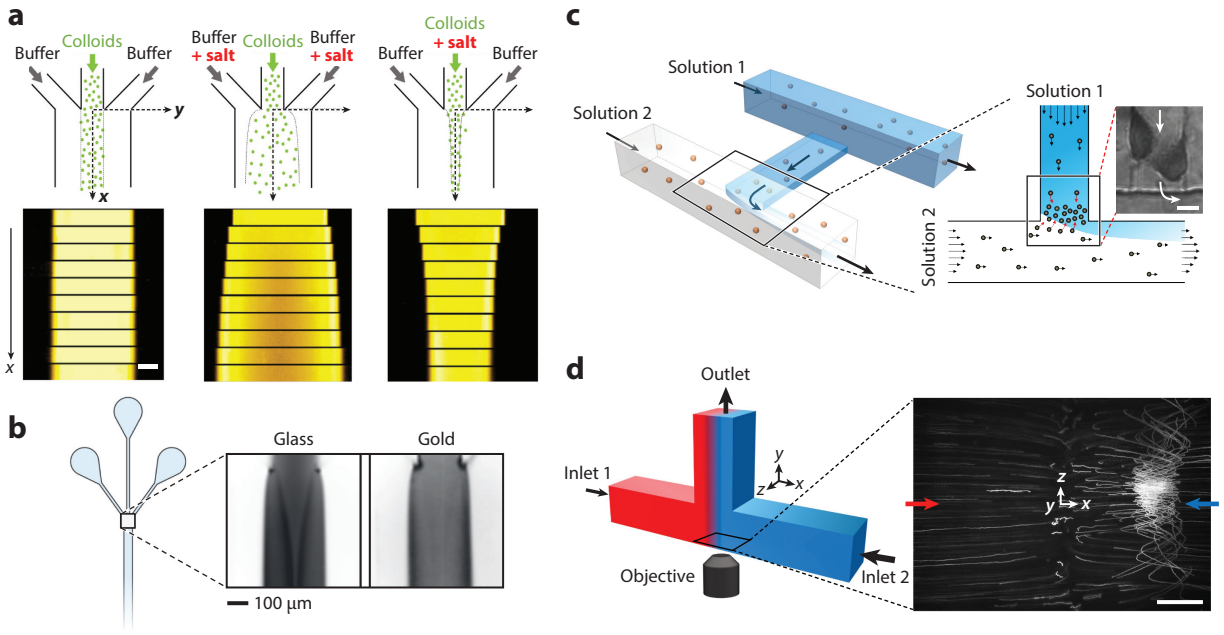

Figure 6

Diffusiophoresis in merging flow systems. (*a*) Ψ-shaped channel designed to introduce cross-stream solute gradients along the downstream. When the outer streams contain salt, the particles in the middle stream experience diffusiophoresis in the direction transverse to the flow. The bottom panels are fluorescence images of colloidal particles taken along the downstream direction. The scale bar represents 50 μm. (*b*) Ψ-shaped channel showing out-of-plane swirling diffusiophoresis effects depending on the channel surface charge. (*c*) Merging T-junctions in a microfluidic channel showing sharp solute gradients that compete with fluid advection in the connecting channel, resulting in particle trapping. The scale bar in the inset represents 20 μm. (*d*) Symmetric merging T-junction experiencing near-wall diffusiophoretic particle trapping near the stagnation point. The scale bar represents 100 μm. Panel *a* adapted with permission from Abécassis et al. (2008). Panel *b* adapted with permission from Migacz et al. (2023). Panel *c* adapted from Shin et al. (2017b) (CC BY 4.0). Panel *d* adapted from Shin et al. (2020) (CC BY 4.0).

particles. For example, in the original demonstration of this system, particles with positive mobility to salt were injected in the center inlet and a buffer solution through both side inlets. Salt was added to either the center inlet or both side inlets, and control was performed without salt. In the control case, the particle stream simply diffused slowly as it was advected downstream (**Figure 6*a***, left). However, when salt was added to the outer inlets, the particle stream experienced a clear broadening effect (**Figure 6*a***, middle), whereas when salt was added to the center inlet, the particle stream was strongly focused as it progressed downstream (**Figure 6*a***, right).

While the natural approach that has been used to investigate/model these systems is with a top-down, 2D analysis, in fact the dispersion and diffusioosmosis in such systems can introduce complex 3D structures to the particle dynamics. The transverse solute gradients can create vortical flows that lead to spiral-like particle distribution (Migacz et al. 2023) (**Figure 6*b***). This is effectively identical to the osmotic dispersion shown in **Figure 5*c***, except with time replaced by the axial flow coordinate, and thus analogies can be made to the dispersion works referenced in Section 3.1.2.

Another example is by the introduction of 3D out-of-plane structures downstream of the junction. For example, when an array of dead-end pore microgrooves is added in the depth direction of the channel, the out-of-plane solute gradient drives diffusiophoresis that sets up a

reversible particle trapping near the entrance of the grooves (Singh et al. 2020). Interestingly, in this configuration, the background fluid flow and diffusiophoresis never exactly balance, leading to appreciable but limited particle focusing that prevents permanent particle clogging and facilitates the reversibility of the trapping.

3.2.2. Merging T-junctions. As is the case for Ψ-shaped channels, T-junctions represent another platform for investigating diffusiophoresis in merging flows. As a simple illustration, consider two parallel flow streams that are connected by a narrow pore so that T-junctions are formed at the intersection of the interconnecting pore and the flow channels (**Figure 6*c***). Supposing that both flow streams carry different solute concentrations and have a pressure imbalance from one side to the other, a net flow will build up in the connecting pore, along with diffusion of the solute from the high-concentration side to the other. When particles are present in the system inside the connecting pore, they will experience the combined effects of flow and diffusiophoresis near the T-junction, which may act in concert or in opposition to each other, depending on the particle mobility. When these effects act in concert, the system will exhibit an enhanced pumping of particles from one channel to the other, but when they act in opposition, the particles will migrate through the pore against the flow until advection and diffusiophoresis balance, at which point they will rapidly accumulate, potentially even approaching the packing limit of the particles (Shin et al. 2017b) (**Figure 6*c***). Because the mean flow velocity in the connecting pore is approximately independent of position in the pore, whereas the diffusiophoretic velocity varies throughout the pore via its dependence on the solute concentration gradient, the location where these two effects balance depends largely on the particle mobility (Ault et al. 2018).

Several simple modifications of this system are possible to achieve different effects. For example, by maintaining a perfect pressure balance across the two channels, the pressure-driven flow in the pore can be suppressed such that diffusiophoresis will continuously pump particles from one side to the other. Using tapered pores, the solute concentration profile in the pore is altered, which in turn provides a mechanism to control the diffusiophoresis and diffusioosmosis in the pore to locally balance each other out (Rasmussen et al. 2020, Jotkar & Cueto-Felgueroso 2021).

These flow geometries also provide further opportunities for different flow configurations, each of which has potential utility for investigating different aspects of the coupled transport. For example, the merging of two contrasting solute streams at a symmetric T-junction has been shown to exhibit spontaneous trapping of particles in a near-wall vortex near the stagnation point(s) that result(s) from a balance of the transport processes (Shin et al. 2020) (**Figure 6*d***). These trapping dynamics arise out of a complex interaction between particle diffusiophoresis, diffusioosmosis at the channel walls, and background merging flow of the mixing streams. An important aspect of this trapping phenomenon is the fact that it is a very near-wall behavior that is best visualized when looked at from the side of the channel, rather than the typical top-down approach of standard microfluidics, which suggests that such dynamics may be going unobserved in other systems involving merging solute streams.

3.3. Diffusiophoresis in Vortical/Turbulent Flows

Finally, the coupling of particle diffusiophoresis with background flows has been considered in the presence of vortical and even turbulent background flows. Such flows can rapidly stretch and fold a solute patch into elongated fibrous structures, thus providing more microscopic solute gradients for diffusiophoresis to occur. For example, by introducing a small amount of salt as a co-mixing species in a herringbone micromixer, Deseigne et al. (2014) showed that the chaotic mixing of particles can be effectively enhanced or inhibited (**Figure 7*a***), illustrating how the relatively weak and small-scale diffusiophoresis can couple across length scales to alter the macroscale mixing

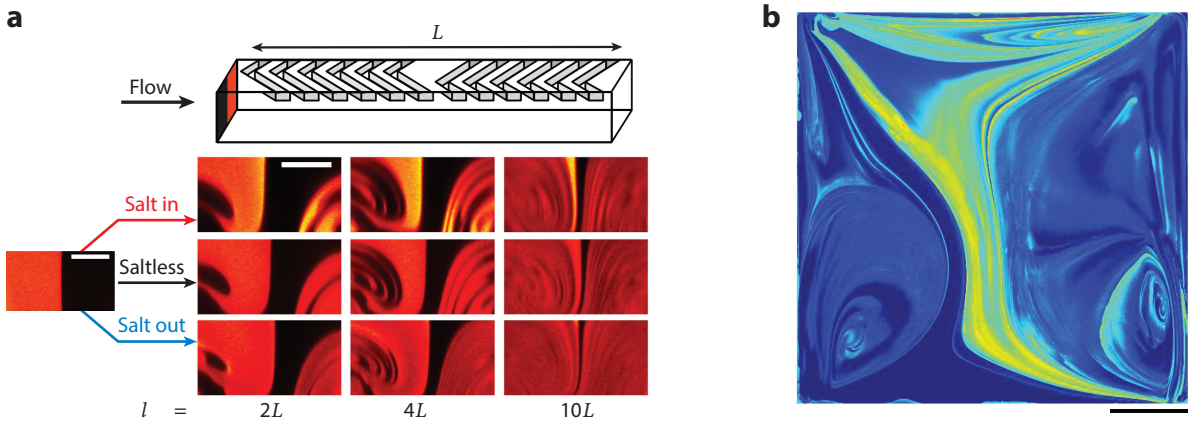

Figure 7

Diffusiophoresis in chaotic mixing systems. (*a*) Enhanced or inhibited colloidal mixing in herringbone micromixers by diffusiophoresis. The scale bar represents 50 μm. (*b*) Chaotic mixing in a Hele–Shaw cell where four corners provide random fluctuating flows. The scale bar represents 1 cm. Panel *a* adapted with permission from Deseigne et al. (2014). Panel *b* adapted with permission from Mauger et al. (2016).

dynamics at much larger length scales. Mauger et al. (2016) considered the role of diffusiophoresis in the macroscale mixing of colloids in chaotic fluid flows by exploring the mixing dynamics in a square Hele–Shaw cell with a time-periodic fluid forcing and mixing protocol (**Figure 7*b***). They introduced an effective Péclet number to quantify the averaged impact of the diffusiophoresis on the overall mixing, and they performed a scale-by-scale analysis to investigate how the effects of diffusiophoresis affect each scale of the concentration field dynamics.

Building on these ideas, Shukla et al. (2017) considered how the transport of colloidal particles in a turbulent flow can be altered by diffusiophoresis, by introducing a Gaussian-distributed patch of solute that decays and is mixed by the turbulence. In turn, this solute drives diffusiophoresis of particles toward or away from the center of the patch, and the overall effect is governed by a single dimensionless number characterizing the balance between turbulent dispersion and compressibility of the particle concentration field. Related works investigated the joint dispersion of initially Gaussian-distributed solute and colloid distributions in linear flows and how the coupling of the two can enhance or inhibit the spreading of the colloidal patch (Raynal et al. 2018, Raynal & Volk 2019). In the salt-attracting case, the peak colloid concentration does not depend on the flow-stretching rate in either strain or shear flows, but rather only on the diffusivities of the salt and colloids and the diffusiophoretic mobility. In the case of pure deformation, the diffusiophoresis modifies the Batchelor scale in a predictable way that can be characterized with an effective Péclet number (Raynal et al. 2018, Raynal & Volk 2019). Furthermore, the mixing time is delayed in the salt-attracting configuration and enhanced in the salt-repelling configuration.

Volk et al. (2022) studied the mixing/demixing/dispersion of both salt and diffusiophoretic colloids in a 2D cellular vortical flow with closed streamlines with an externally imposed salt gradient. Here, they considered how the long-timescale mean particle velocity and effective diffusivity depend on the diffusiophoretic coupling between the particles and the salt gradient. They defined a blockage criterion capturing the relative influence of diffusiophoresis and diffusion. When diffusiophoresis is relatively weak, the mean velocity of cell-to-cell particle travel is enhanced by diffusiophoresis, but when the diffusiophoresis is strong enough, it leads to particle depletion at the separatrices between cells, effectively preventing cell-to-cell particle transport.

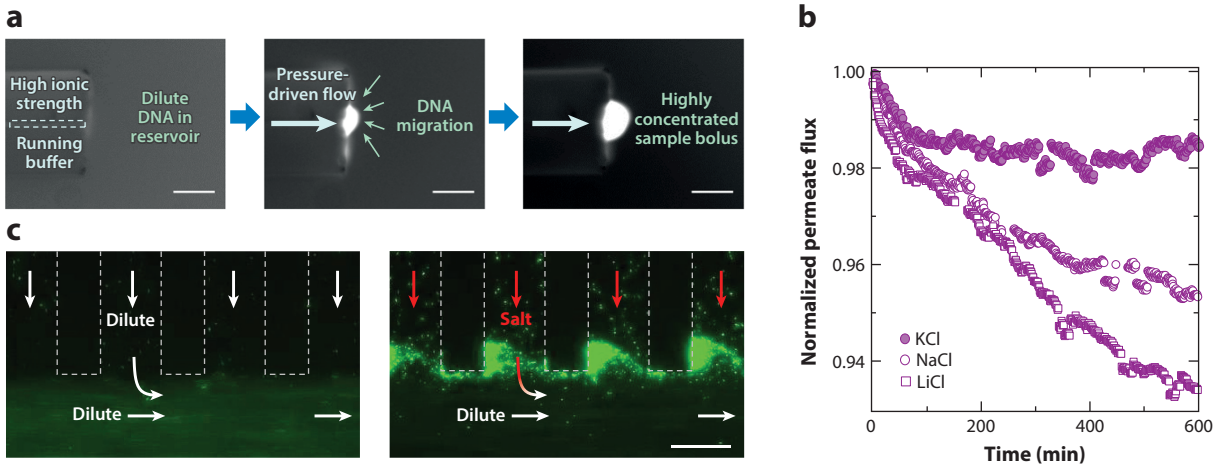

Figure 8

Colloidal accumulation by diffusiophoresis in merging flow systems. (*a*) Accumulation of DNA by flowing a stream of high-ionic-strength buffer to the reservoir of dilute DNA. (*b*) Decline of permeate flux across reverse osmosis membranes due to fouling by particles suspended in different salt solutions. (*c*) Buildup of *Escherichia coli* in the junctions of merging streams of different salinity. The left panel indicates no salinity difference between the two streams, whereas the right panel shows when the upper stream is more saline than the lower stream. The scale bars in panels *a* and *c* represent 50 μm. Panel *a* adapted from Friedrich et al. (2017) (CC BY 4.0). Panel *b* adapted with permission from Guha et al. (2015). Panel *c* adapted from Doan et al. (2020) (CC BY 4.0).

4. DIFFUSIOPHORESIS IN NATURAL AND PRACTICAL SYSTEMS

So far, we have discussed how diffusiophoresis coupled with background flows can cause intriguing colloidal transport. It is no surprise that diffusiophoresis can be observed in a wide range of natural and artificial systems involving fluid flows. In this section, we briefly introduce recent studies that discuss how diffusiophoresis may arise and play crucial roles in engineering and biological systems, and we also demonstrate diffusiophoresis as a tool to achieve some useful applications, such as separation, hydrocarbon recovery, drug delivery, and coating.

4.1. Diffusiophoresis in Channel Flows

As discussed in Sections 3.1 and 3.2, diffusiophoresis can lead to continuous segregation or trapping of colloidal particles in straight and merging flow channels. While these effects can enable useful applications like separation (**Figures 5*a*** and **8*a***), they can also cause detrimental effects, such as clogging in filtration and flow systems (**Figure 8*b*,*c***).

4.1.1. Particle separation. Field-flow fractionation is a flow-based separation technique that is commonly achieved in microfluidic flows. This method involves the migration of particles across the flow streamlines by external fields transverse to the flow direction in laminar flows (Giddings 1993). In this regard, the ability to direct the motion of stable micro-/nanoscale particles makes diffusiophoresis an attractive method for portable separation applications without the need for additional equipment to provide external forces. Directing particles across streamlines by diffusiophoresis in such settings requires establishing solute gradients transverse to the flow. As discussed in Section 3.2.1, this can be achieved by coflowing multiple streams of different solute compositions (Abécassis et al. 2008, Chakra et al. 2023) (**Figure 6*a***) or establishing transverse solute gradients by chemical reactions using, e.g., gas dissolution (Shin et al. 2017c, Shimokusu et al. 2020) (**Figure 5*a***) or ion exchange (Lee et al. 2018, Seo et al. 2020). In these systems, Pe_p is

the relevant dimensionless number that serves as the basis for the design of flow-based diffusiophoretic separation where particles of different mobility (e.g., particle size, shape, surface charge) can be separated.

Another approach to establishing a steady-state solute concentration gradient in the presence of a background flow for continuous particle separation is to inject fluid of one solute concentration through a channel into a reservoir (either a stream or a stagnant bath) of another solute concentration where particles may migrate against the flow direction, a scenario similar to the T-junction described in Section 3.2.2. For example, Friedrich et al. (2017) showed that when injecting a high-ionic-strength solution into a reservoir containing a low-ionic-strength solution and dilute DNA, the negatively charged DNA will be pulled toward the tip of the microcapillary via diffusiophoresis, where DNA molecules will encounter the outflow from the tube. These two effects will balance near the tip, leading to rapid DNA focusing (**Figure 8*a***). The key advantage of this configuration is that the fluid advection can establish sharp, steady-state concentration gradients that enable rapid colloid accumulation at a fixed location, which is often required to elevate the concentration of dilute biosamples for reliable detection and analysis. Recent studies have shown preconcentration and separation of DNA of varying lengths (Friedrich et al. 2017, Li et al. 2020, Katzmeier & Simmel 2024) and exosomes of varying sizes and compositions (Rasmussen et al. 2020).

Other options are available to drive the counteracting fluid flow and solute gradients. Methods to induce fluid flow include using evaporation (D. Lee et al. 2020) and imbibition (Lee & Kim 2020) in nanoporous media. Both methods have the advantage of not requiring external power sources or other peripheral devices to drive the dynamics, making them suitable for portable, low-cost sensing applications.

In addition to diffusiophoresis, the native surface charge on microfluidics channel walls (PDMS, glass, polymethyl methacrylate, etc.) inevitably introduces diffusioosmosis, providing additional transport modes to the particle motion since the directions of wall diffusioosmosis and particle diffusiophoresis may not be parallel to each other in flow systems with complex channel geometries. This can enable more sophisticated separation with a higher degree of freedom (Shin et al. 2020, Singh et al. 2020, Migacz et al. 2023).

It should be noted that the major drawback of using diffusiophoresis for separation is the addition of external solute molecules, which is often undesired for downstream analysis or for colloids that are vulnerable to the changes in the chemistry of the background (cells, proteins, viruses, nucleic acids, etc.). Introducing easy-to-separate solute can be an alternative strategy to overcome such limitations. Examples include soluble gases, such as CO_2 and ammonia, which are also commonly used in forward osmosis desalination due to their high solubility and ease of removal (McCutcheon et al. 2005). The sequence of particle separation followed by gas removal can be further utilized in a repeating fashion to improve efficiency and throughput.

4.1.2. Membrane fouling. While diffusiophoresis in channel flows can enable cross-stream particle separation, the same principle can also lead to clogging in the context of membrane-based filtration. Membrane-based filtration that involves nanoporous membranes, such as ultrafiltration and reverse osmosis (RO) membranes, naturally creates a solute boundary layer over the membrane. Guha et al. (2015) showed that when microscale particulates are present in saline feed water, diffusiophoresis can accelerate the clogging of the RO membrane. This is shown to be particularly sensitive to the types of solutes present in the feed water, where the solute yielding larger diffusiophoretic mobility led to faster clogging (**Figure 8*b***). Shin et al. (2017b) demonstrated that diffusiophoresis arising in merging channel flows can cause small colloidal particles to clog channels that are orders of magnitude larger than the particles (**Figure 6*c***). This effect is also shown

to accelerate the formation of bacterial biofilms at flow junctions (Doan et al. 2020) (**Figure 8*c***). These observations suggest the role of diffusiophoresis in the clogging of a broad class of filtration membranes and flow networks.

4.2. Diffusiophoresis in Porous Media

Due to the reduced hydrodynamic particle–wall interactions, diffusiophoresis potentially offers an effective way to manipulate colloidal particles in tightly confined porous media, including subsurface aquifers, biological tissues, and woven fabrics. Relevant applications in the context of colloidal transport in such systems include oil recovery, drug delivery, and fabric cleaning.

4.2.1. Enhanced oil recovery. Diffusiophoresis also has been a recurring subject in the context of enhanced oil recovery (EOR) (Kar et al. 2015, Prieve et al. 2019, Park et al. 2021, Shi & Abdel-Fattah 2021). Extracting hydrocarbons from a subsurface reservoir involves injecting seawater or brine water into the connate subsurface, followed by flooding with additional engineered water to further extract the remaining oil from the reservoir. As discussed in Section 3.1.3, diffusiophoresis can affect the particle motion in dead-end pores, which make up a considerable portion of the pore space in various types of subsurface reservoirs. Using a reservoir-mimicking microfluidic device, Park et al. (2021) showed that this geometrical feature of subsurface reservoirs leads to salinity-dependent oil recovery efficiency, suggesting the role of diffusiophoresis during chemical flooding.

Low-salinity water flooding, one of the recently developed EOR processes, is a counterintuitive chemical flooding process in which a solution of reduced salinity is injected into the subsurface. While this method has shown some success, it has been a frequent source of debate over the past decade in terms of its effectiveness and mechanism where there have been inconsistent reports from lab and field tests (Sheng 2014, Tetteh et al. 2020). One of the overlooked aspects of the EOR process affected by the salinity change is pore-scale transport. Low-salinity water flooding naturally creates salinity gradients at the pore scale, causing diffusiophoresis to arise (Kar et al. 2015, Prieve et al. 2019, Park et al. 2021). From the pore-scale transport aspect, it was shown that diffusiophoresis induced by low-salinity water flooding is in fact not in favor of oil recovery due to the direction of diffusiophoresis generally being into the pores containing high-salinity brine for negatively charged oil droplets (Park et al. 2021). However, other pertinent effects, such as Marangoni flows (Maass et al. 2016), charge reversal with multivalent ions (Grosberg et al. 2002), and diffusioosmotic pumping (Marbach & Bocquet 2019), can act favorably for recovering oil via low-salinity water flooding, thus warranting further studies.

4.2.2. Drug delivery. Another potential application of using diffusiophoresis for delivering colloidal particles in confined porous media is drug delivery in biological tissues such as tumors (Doan et al. 2021) and biofilms (Somasundar et al. 2023). Biological tissues are generally porous, and some are characterized by extremely tight confinement when compressed. Compressed tissues are one of the key hallmarks of tumors, where the confinement arises due to abnormal cell growth, causing tighter interstitial space between the cells (Jain et al. 2014). The high collagen activity also contributes to additional confinement within the interstitium (Provenzano et al. 2008). These conditions impose a challenge in drug delivery where therapeutic nanoparticles must navigate across the confined interstitium.

While studies have shown that drug-encapsulated micro-/nanomotors can be delivered in vivo actively via self-diffusiophoretic propulsion (de Ávila et al. 2017, Tang et al. 2020), a swarm of drug nanoparticles undergoing passive diffusiophoresis along a predetermined direction can be an alternative, feasible method to enhance their transport across compressed tissues. To succeed,

one needs to establish chemical gradients across the tissue, which may be achieved through intravenous delivery of different chemical compositions while maintaining the overall osmolarity [e.g., Ringer's solution (Alexander et al. 2009)]. For instance, recent demonstrations showed that the diffusiophoretic delivery of therapeutic nanoparticles and liposomes into confined spaces can be achieved at isotonic conditions by exchanging saline solution with glucose (Shin et al. 2019, Doan et al. 2021).

4.2.3. Other applications. Another practical application involving porous media where diffusiophoresis plays an important role is laundry detergency for cleaning fabrics. While it has been naively believed that the water flow driven by the washer's churning motion drives dirt out from the fabric, this flow is, in fact, not strong enough to penetrate deep inside individual yarns due to the biporous nature of a woven fabric. This leaves behind the so-called stagnant core within the yarn that is devoid of fluid flow. The stagnant core effectively acts as one large dead-end space where Brownian motion is the only apparent transport mechanism for the soil particles residing in this region (Warmoeskerken et al. 2002). In this regard, the exact mechanism of laundry detergency was considered a mystery for many decades. Shin et al. (2018) showed that detergent gradients established during the freshwater rinse can induce diffusiophoresis, allowing soil particles to escape from the stagnant core. The logarithmic nature of electrolytic diffusiophoresis (i.e., $\mathbf{u}_p \sim \nabla \ln c_\infty$) prolongs the lifetime of diffusiophoresis due to the reduced surfactant concentration during the freshwater rinse. Such logarithmic diffusiophoresis is also shown to enable other applications involving confined geometries, such as colloidal patterning (Palacci et al. 2010), particle delivery to hidden targets (Tan et al. 2021), and maze solving (Gandhi et al. 2020).

4.3. Diffusiophoresis During Drying

Evaporation of colloidal films often causes an uneven distribution of colloidal particles near the interface, which may lead to particle stratification (Fortini et al. 2016). Sear & Warren (2017) investigated the role of diffusiophoresis in the segregation of small particles from large particles during the drying of colloidal films. It was predicted that whether the small particles emerge on top of the larger ones (small-on-top stratification) or vice versa (large-on-top stratification) depends on the evaporation rate u_e (characterized through the drying Péclet number $\mathrm{Pe}_d = u_e H/D_p$, where H is the initial film thickness and D_p is the diffusivity of large particles) and the initial concentration of small particles ϕ_0 (which act as solute particles), where fast evaporation and high particle concentration drive diffusiophoresis of large particles away from the small particles (**Figure 9*a***). Recent experimental studies have also shown good agreement with such theoretical predictions (Schulz et al. 2020).

For drying of sessile drops, the pinning of a three-phase contact line leads to the buildup of colloidal rings (so-called coffee rings) (Deegan et al. 1997). Guha et al. (2017) showed that the formation of coffee rings can be controlled by diffusiophoresis, which was utilized to achieve uniform coating as well as to separate DNA (**Figure 9*b***). On a related note, Ghosh et al. (2023) demonstrated the impact of diffusiophoresis on drying patterns by controlling the atmosphere with either CO_2 or N_2 and discussed that diffusiophoresis could potentially offer versatile control over the particle deposition quality in additive manufacturing processes (**Figure 9*c***). Boulogne et al. (2017) showed that diffusiophoresis could force the particles to coat on the substrate prior to the complete evaporation of the solvent when deposited on solute-releasing surfaces (e.g., hydrogels), leading to uniform coating free of coffee rings.

Another configuration of colloidal drying is solvent evaporation occurring in an open capillary filled with colloidal suspension. Xu et al. (2023) showed that when the capillary is laid horizontally, the evaporation at the open end of the capillary establishes solute concentration gradients

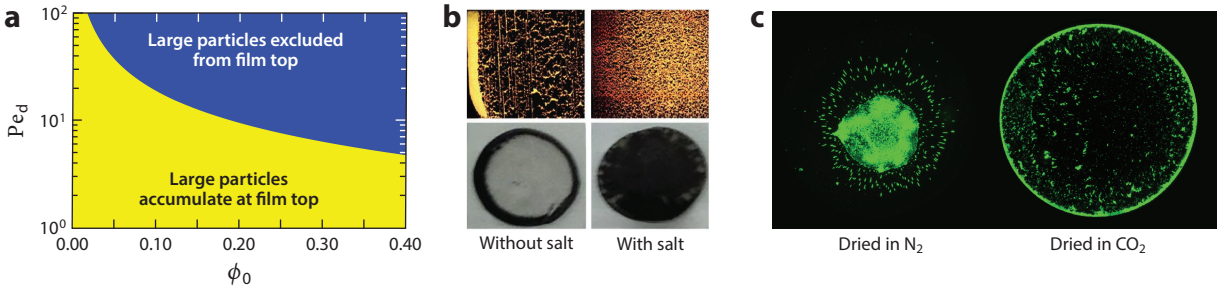

Figure 9

Effect of diffusiophoresis on drying of colloidal suspensions. (*a*) A phase diagram depicting the particle configuration during drying of planar colloidal films. Pe_d and ϕ_0 are the drying Péclet number and the initial concentration of the solute particles, respectively. (*b*) Drying marks of sulfate-modified polystyrene particles (*top*) and carbon nanotubes (*bottom*) in the absence (*left*) or presence (*right*) of salt (potassium hydrogen phthalate). (*c*) Drying marks of amine-modified polystyrene particles after drying in N_2 (*left*) and CO_2 (*right*) atmospheres. Panel *a* adapted with permission from Sear & Warren (2017). Panel *b* adapted with permission from Guha et al. (2017). Panel *c* adapted with permission from Ghosh et al. (2023).

and drives particle diffusiophoresis toward or away from the interface depending on the particle mobility. In addition, evaporation may set up a density difference in the suspension that drives a gravity-driven recirculation from the open end, which can impact the dispersion of the particles. The authors modeled these coupled dynamics using a similar derivation of a 1D macrotransport theory used in hydrodynamic dispersions as mentioned in Section 3.1.2 (Chu et al. 2021, 2022).

4.4. Diffusiophoresis in Biological Systems

Living cells are dynamic, heterogeneous entities that exhibit spatiotemporal thermodynamic gradients to maintain intracellular transport processes crucial to sustaining life. An in vivo investigation performed by Parry et al. (2014) uncovered the metabolic-dependent motion of nanoscale biocolloids (enzyme granules, plasmid, and viral proteins) in *Escherichia coli*, where the distribution of the displacements was shown to be far from Gaussian, indicating the nonuniform nature of the cytoplasm.

While the complexity of the cell makes it experimentally challenging to quantify the chemical heterogeneity of the cytoplasm, theoretical estimations may provide some quantitative insights into the size of the biochemical gradients and whether these gradients can drive diffusiophoresis. For instance, Sear (2019) predicted that the size of adenosine triphosphate (ATP) gradients in *E. coli* could be fairly large ($0.1 \sim 1$ mM/μm) owing to the fast turnaround rate of ATPs in the cytoplasm. These gradients are expected to be strong enough to induce diffusiophoresis of nanoscale colloids with a speed of ~0.1 μm/s. Using in vitro experiments, Ramm et al. (2021) recently showed that the concentration gradients of ATP and ATP-bound proteins in *E. coli* play a role in driving the diffusiophoretic motion of membrane-bound cargo proteins, suggesting the critical role of diffusiophoresis in cell division.

In the context of biomolecular phase separation, an area of active research, biomolecular condensates are inherently associated with chemical gradients due to their heterogeneous nature (Banani et al. 2017). The biomolecular condensates concentrate organelle-specific proteins and nucleic acids in a spatiotemporal manner to achieve their desired functions in the cell. Testa et al. (2021) showed that the enhanced enzymatic activity within the condensate due to the concentrated enzymes resulted in the local concentration gradients of the products, thereby driving interfacial

flow around the condensates akin to diffusioosmosis. Doan et al. (2024) showed that diffusiophoresis can strengthen the phase separation of biomolecular condensates by locally enriching the biomolecular constituents and imparting directional motility to the condensates, thereby impacting their lifetime. A recent study by Jambon-Puillet et al. (2024) showed that active motility could also emerge from enzymatic reactions, leading to phoretic swimming of biomolecular condensates. These latest studies suggest that diffusiophoresis may possibly play a role in the formation and functions of intracellular membraneless organelles.

5. SUMMARY AND OUTLOOK

While diffusiophoresis was first discovered nearly 80 years ago, it is only in the last decade that significant growth in diffusiophoresis research has taken place. This review highlighted some of the recent advances in understanding diffusiophoresis in theoretical, computational, and experimental contexts. We discussed diffusiophoresis at the fundamental level and how diffusiophoresis arises in flow systems. We further reviewed diffusiophoresis in natural and artificial systems and outlined some useful technological applications enabled by diffusiophoresis. Despite substantial developments, there are still many open questions pertinent to the fundamentals and applications of diffusiophoresis left to be explored, some of which are highlighted below.

FUTURE ISSUES

1. While there has been a limited understanding of diffusiophoresis in non-Newtonian fluids (Tseng et al. 2016, Saad & Natale 2019), the colloidal nature of most non-Newtonian fluids suggests that continuum descriptions may not be sufficient to correctly capture solute–particle interactions occurring at the nanoscale, warranting future studies.
2. Apart from theoretical predictions (Marbach et al. 2020, McKenzie et al. 2022), whether diffusiophoresis can induce considerable deformation for viscoelastic biocolloids, such as vesicles, gels, biomolecular condensates, and nucleic acids, is still an open question. If so, diffusiophoresis could possibly be exploited to enable DNA sequencing, protein unfolding, or liposomal drug release.
3. Other higher-order effects not discussed in this review include nonuniform surface properties (Solomentsev & Anderson 1994), reacting particles (Yang et al. 2019), ion steric effects (Stout & Khair 2017), ion correlation effects (Stout & Khair 2014, Gupta et al. 2020a), and nonlinear, multidimensional chemical gradients (Warren 2020, Raj et al. 2023, Williams et al. 2024), many of which still deserve further investigations. Understanding how these effects influence diffusiophoresis may enable novel ways to achieve enhanced separation or colloidal self-assembly (Wang et al. 2022, Shin 2023).
4. While the typical top-down microfluidics approach for studying diffusiophoresis is highly conducive to investigating two-dimensional or depth-averaged systems, the latest research highlights the highly three-dimensional nature of these systems, often even when solute variations on the cross section are relatively small (Shin et al. 2020, Singh et al. 2020, Migacz et al. 2023).
5. While research on diffusiophoresis in mixing and turbulent systems is relatively limited to specific configurations (Deseigne et al. 2014, Shukla et al. 2017, Raynal et al. 2018, Raynal & Volk 2019, Volk et al. 2022), these results nonetheless pave the way for

understanding diffusiophoresis in more complex turbulent flows. Generally, these results suggest that, although diffusiophoresis is a small-scale phenomenon occurring at the microscale, the effects of particle/solute/fluid coupling can cascade from one scale to another, possibly leading to novel dynamics at the macroscale, with potential implications for large-scale systems ranging from industrial mixing processes (Villermaux 2019) to natural ecosystems (Stocker 2012).

DISCLOSURE STATEMENT

The authors are not aware of any affiliations, memberships, funding, or financial holdings that might be perceived as affecting the objectivity of this review.

ACKNOWLEDGMENTS

We thank Henry Chu, Ankur Gupta, and Patrick Warren for their valuable feedback. S.S. thanks the National Science Foundation for partial support under grant 2237177.

LITERATURE CITED

Abécassis B, Cottin-Bizonne C, Ybert C, Ajdari A, Bocquet L. 2008. Boosting migration of large particles by solute contrasts. *Nat. Mater.* 7(10):785–89

Akdeniz B, Wood JA, Lammertink RGH. 2023. Diffusiophoresis and diffusio-osmosis into a dead-end channel: role of the concentration-dependence of zeta potential. *Langmuir* 39(6):2322–32

Akdeniz B, Wood JA, Lammertink RGH. 2024. Diffusiophoresis in polymer and nanoparticle gradients. *J. Phys. Chem. B* 128(24):5874–87

Alessio BM, Gupta A. 2023. Diffusiophoresis-enhanced Turing patterns. *Sci. Adv.* 9(45):eadj2457

Alessio BM, Shim S, Gupta A, Stone HA. 2022. Diffusioosmosis-driven dispersion of colloids: a Taylor dispersion analysis with experimental validation. *J. Fluid Mech.* 942:A23

Alexander M, Corrigan A, Gorski L, Hankins J, Perucca R. 2009. *Infusion Nursing: An Evidence-Based Approach*. St. Louis, MO: Saunders Elsevier Health. 3rd ed.

Anderson JL. 1989. Colloid transport by interfacial forces. *Annu. Rev. Fluid Mech.* 21:61–99

Anderson JL, Lowell ME, Prieve DC. 1982. Motion of a particle generated by chemical gradients Part 1. Non-electrolytes. *J. Fluid Mech.* 117:107–21

Anderson JL, Prieve DC. 1991. Diffusiophoresis caused by gradients of strongly adsorbing solutes. *Langmuir* 7(2):403–6

Antoine EE, Vlachos PP, Rylander MN. 2014. Review of collagen I hydrogels for bioengineered tissue microenvironments: characterization of mechanics, structure, and transport. *Tissue Eng. Part B Rev.* 20(6):683–96

Ault JT, Shin S, Stone HA. 2018. Diffusiophoresis in narrow channel flows. *J. Fluid Mech.* 854:420–48

Ault JT, Warren PB, Shin S, Stone HA. 2017. Diffusiophoresis in one-dimensional solute gradients. *Soft Matter* 13(47):9015–23

Banani SF, Lee HO, Hyman AA, Rosen MK. 2017. Biomolecular condensates: organizers of cellular biochemistry. *Nat. Rev. Mol. Cell Biol.* 18(5):285–98

Battat S, Ault JT, Shin S, Khodaparast S, Stone HA. 2019. Particle entrainment in dead-end pores by diffusiophoresis. *Soft Matter* 15(19):3879–85

Bhaskar B, Bhattacharyya S. 2023. Diffusiophoresis of a highly charged rigid colloid in a hydrogel incorporating ion steric interactions. *Phys. Fluids* 35(10):102023

Bishop KJM, Biswal SL, Bharti B. 2023. Active colloids as models, materials, and machines. *Annu. Rev. Chem. Biomol. Eng.* 14:1–30

Boulogne F, Shin S, Dervaux J, Limat L, Stone HA. 2017. Diffusiophoretic manipulation of particles in a drop deposited on a hydrogel. *Soft Matter* 13(30):5122–29

Brady JF. 2011. Particle motion driven by solute gradients with application to autonomous motion: continuum and colloidal perspectives. *J. Fluid Mech.* 667:216–59

Chakra A, Singh N, Vladisavljevic GT, Nadal F, Cottin-Bizonne C, et al. 2023. Continuous manipulation and characterization of colloidal beads and liposomes via diffusiophoresis in single-and double-junction microchannels. *ACS Nano* 17(15):14644–57

Chang YC, Keh HJ. 2008. Diffusiophoresis and electrophoresis of a charged sphere perpendicular to two plane walls. *J. Colloid Interface Sci.* 322(2):634–53

Chen PY, Keh HJ. 2005. Diffusiophoresis and electrophoresis of a charged sphere parallel to one or two plane walls. *J. Colloid Interface Sci.* 286(2):774–91

Chiang TY, Velegol D. 2014. Multi-ion diffusiophoresis. *J. Colloid Interface Sci.* 424:120–23

Chiu HC, Keh HJ. 2017. Diffusiophoresis of a charged particle in a microtube. *Electrophoresis* 38(19):2468–78

Chu HCW, Garoff S, Tilton RD, Khair AS. 2021. Macrotransport theory for diffusiophoretic colloids and chemotactic microorganisms. *J. Fluid Mech.* 917:A52

Chu HCW, Garoff S, Tilton RD, Khair AS. 2022. Tuning chemotactic and diffusiophoretic spreading via hydrodynamic flows. *Soft Matter* 18(9):1896–910

de Ávila BEF, Angsantikul P, Li J, Angel Lopez-Ramirez M, Ramírez-Herrera DE, et al. 2017. Micromotor-enabled active drug delivery for in vivo treatment of stomach infection. *Nat. Commun.* 8(1):272. Erratum. 2017. *Nat. Commun.* 8(1):1299

Deegan RD, Bakajin O, Dupont TF, Huber G, Nagel SR, Witten TA. 1997. Capillary flow as the cause of ring stains from dried liquid drops. *Nature* 389(6653):827–29

Derjaguin BV, Dukhin SS, Korotkova AA. 1961. Diffusiophoresis in electrolyte solutions and its role in the mechanism of the formation of films from caoutchouc latexes by the ionic deposition method. *Colloid J. USSR* 23(1):53–58

Derjaguin BV, Sidorenkov GP, Zubashchenkov EA, Kiseleva EV. 1947. Kinetic phenomena in boundary films of liquids. *Colloid J. USSR* 9:335–47

Deseigne J, Cottin-Bizonne C, Stroock AD, Bocquet L, Ybert C. 2014. How a "pinch of salt" can tune chaotic mixing of colloidal suspensions. *Soft Matter* 10(27):4795–99

Doan VS, Alshareedah I, Singh A, Banerjee PR, Shin S. 2024. Diffusiophoresis promotes phase separation and transport of biomolecular condensates. *Nat. Commun.* 15(1):7686

Doan VS, Chun S, Feng J, Shin S. 2021. Confinement-dependent diffusiophoretic transport of nanoparticles in collagen hydrogels. *Nano Lett.* 21(18):7625–30

Doan VS, Kim DO, Snoeyink C, Sun Y, Shin S. 2023. Shape- and orientation-dependent diffusiophoresis of colloidal ellipsoids. *Phys. Rev. E* 107(5):L052602

Doan VS, Saingam P, Yan T, Shin S. 2020. A trace amount of surfactants enables diffusiophoretic swimming of bacteria. *ACS Nano* 14(10):14219–27

Dukhin SS. 1993. Non-equilibrium electric surface phenomena. *Adv. Colloid Interface Sci.* 44:1–134

Ebel JP, Anderson JL, Prieve DC. 1988. Diffusiophoresis of latex particles in electrolyte gradients. *Langmuir* 4(2):396–406

Florea D, Musa S, Huyghe JMR, Wyss HM. 2014. Long-range repulsion of colloids driven by ion exchange and diffusiophoresis. *PNAS* 111(18):6554–59

Fortini A, Martín-Fabiani I, De La Haye JL, Dugas PY, Lansalot M, et al. 2016. Dynamic stratification in drying films of colloidal mixtures. *Phys. Rev. Lett.* 116(11):118301. Erratum. 2016. *Phys. Rev. Lett.* 116:229902

Friedrich SM, Burke JM, Liu KJ, Ivory CF, Wang TH. 2017. Molecular rheotaxis directs DNA migration and concentration against a pressure-driven flow. *Nat. Commun.* 8(1):1213

Gandhi T, Huang JM, Aubret A, Li Y, Ramananarivo S, et al. 2020. Decision-making at a T-junction by gradient-sensing microscopic agents. *Phys. Rev. Fluids* 5(10):104202

Ganguly A, Roychowdhury S, Gupta A. 2024. Unified mobility expressions for externally driven and self-phoretic propulsion of particles. *J. Fluid Mech.* 994:A2

Ghosh S, Lee S, Johnson MV, Hardin J, Doan VS, et al. 2023. Diffusiophoresis-enhanced particle deposition for additive manufacturing. *MRS Commun.* 13(6):1053–62

Giddings JC. 1993. Field-flow fractionation: analysis of macromolecular, colloidal, and particulate materials. *Science* 260(5113):1456–65

Grosberg AY, Nguyen TT, Shklovskii BI. 2002. The physics of charge inversion in chemical and biological systems. *Rev. Mod. Phys.* 74(2):329

Groves R, Welche P, Routh AF. 2023. The coagulant dipping process of nitrile latex: investigations of former motion effects and coagulant loss into the dipping compound. *Soft Matter* 19(3):468–82

Guha R, Mohajerani F, Mukhopadhyay A, Collins MD, Sen A, Velegol D. 2017. Modulation of spatiotemporal particle patterning in evaporating droplets: applications to diagnostics and materials science. *ACS Appl. Mater. Interfaces* 9(49):43352–62

Guha R, Shang X, Zydney AL, Velegol D, Kumar M. 2015. Diffusiophoresis contributes significantly to colloidal fouling in low salinity reverse osmosis systems. *J. Membrane Sci.* 479:67–76

Gupta A, Rajan AG, Carter EA, Stone HA. 2020a. Ionic layering and overcharging in electrical double layers in a Poisson-Boltzmann model. *Phys. Rev. Lett.* 125(18):188004

Gupta A, Rallabandi B, Stone HA. 2019. Diffusiophoretic and diffusioosmotic velocities for mixtures of valence-asymmetric electrolytes. *Phys. Rev. Fluids* 4(4):043702

Gupta A, Shim S, Stone HA. 2020b. Diffusiophoresis: from dilute to concentrated electrolytes. *Soft Matter* 16(30):6975–84

Happel J, Brenner H. 1983. *Low Reynolds Number Hydrodynamics: With Special Applications to Particulate Media*, Vol. 1. Hingham, MA: Kluwer

Hsu JP, Ko IF, Tseng S. 2012. Importance of boundary effect on the diffusiophoretic behavior of a charged particle in an electrolyte medium. *J. Phys. Chem. C* 116(7):4455–64

Ishikawa T. 2024. Fluid dynamics of squirmers and ciliated microorganisms. *Annu. Rev. Fluid Mech.* 56:119–45

Israelachvili JN. 2011. *Intermolecular and Surface Forces*. Burlington, MA: Academic. 3rd ed.

Jain RK, Martin JD, Stylianopoulos T. 2014. The role of mechanical forces in tumor growth and therapy. *Annu. Rev. Biomed. Eng.* 16:321–46

Jambon-Puillet E, Testa A, Lorenz C, Style RW, Rebane AA, Dufresne ER. 2024. Phase-separated droplets swim to their dissolution. *Nat. Commun.* 15(1):3919

Jana S, Um SH, Jung S. 2012. Paramecium swimming in capillary tube. *Phys. Fluids* 24(4):041901

Johansson L, Löfroth JE. 1993. Diffusion and interaction in gels and solutions. 4. Hard sphere Brownian dynamics simulations. *J. Chem. Phys.* 98(9):7471–79

Joo SW, Lee SY, Liu J, Qian S. 2010. Diffusiophoresis of an elongated cylindrical nanoparticle along the axis of a nanopore. *ChemPhysChem* 11(15):3281–90

Jotkar M, Cueto-Felgueroso L. 2021. Particle separation through diverging nanochannels via diffusiophoresis and diffusioosmosis. *Phys. Rev. Appl.* 16(6):064067

Jotkar M, de Anna P, Dentz M, Cueto-Felgueroso L. 2024. The impact of diffusiophoresis on hydrodynamic dispersion and filtration in porous media. *J. Fluid Mech.* 991:A8

Kar A, Chiang TY, Rivera IO, Sen A, Velegol D. 2015. Enhanced transport into and out of dead-end pores. *ACS Nano* 9(1):746–53

Katzmeier F, Simmel FC. 2024. Reversible self-assembly of nucleic acids in a diffusiophoretic trap. *Angew. Chem. Int. Ed.* 63(16):e202317118

Keh HJ. 2016. Diffusiophoresis of charged particles and diffusioosmosis of electrolyte solutions. *Curr. Opin. Colloid Interface Sci.* 24:13–22

Keh HJ, Anderson JL. 1985. Boundary effects on electrophoretic motion of colloidal spheres. *J. Fluid Mech.* 153:417–39

Keh HJ, Chen SB. 1988. Electrophoresis of a colloidal sphere parallel to a dielectric plane. *J. Fluid Mech.* 194:377–90

Keh HJ, Hsu LY. 2008. Diffusioosmosis of electrolyte solutions in fibrous porous media. *Microfluid. Nanofluid.* 5(3):347–56

Keh HJ, Hsu LY. 2009. Diffusioosmotic flow of electrolyte solutions in fibrous porous media at arbitrary zeta potential and double-layer thickness. *Microfluid. Nanofluid.* 7(6):773

Keh HJ, Wei YK. 2000. Diffusiophoretic mobility of spherical particles at low potential and arbitrary double-layer thickness. *Langmuir* 16(12):5289–94

Kirby BJ, Hasselbrink EF. 2004. Zeta potential of microfluidic substrates: 1. Theory, experimental techniques, and effects on separations. *Electrophoresis* 25(2):187–202
Kozak MW, Davis EJ. 1986. Electrokinetic phenomena in fibrous porous media. *J. Colloid Interface Sci.* 112(2):403–11
Lee D, Kim J, Lee H, Kim SJ. 2020. Effect of evaporation through nanoporous medium on diffusiophoresis. *Micro Nano Syst. Lett.* 8(1):7
Lee D, Kim SJ. 2020. Spontaneous diffusiophoretic separation in paper-based microfluidic device. *Micro Nano Syst. Lett.* 8:6
Lee E, Lee YS, Yen FY, Hsu JP. 2000. Electroosmotic flow of a general electrolyte solution through a fibrous medium. *J. Colloid Interface Sci.* 223(2):223–28
Lee H, Kim J, Yang J, Seo SW, Kim SJ. 2018. Diffusiophoretic exclusion of colloidal particles for continuous water purification. *Lab Chip* 18(12):1713–24
Lee K, Lee J, Ha D, Kim M, Kim T. 2020. Low-electric-potential-assisted diffusiophoresis for continuous separation of nanoparticles on a chip. *Lab Chip* 20(15):2735–47
Lee S, Lee J, Ault JT. 2023. The role of variable zeta potential on diffusiophoretic and diffusioosmotic transport. *Colloids Surf. A* 659:130775
Lee SY, Yalcin SE, Joo SW, Baysal O, Qian S. 2010. Diffusiophoretic motion of a charged spherical particle in a nanopore. *J. Phys. Chem. B* 114(19):6437–46
Li S, Li A, Hsieh K, Friedrich SM, Wang TH. 2020. Electrode-free concentration and recovery of DNA at physiologically relevant ionic concentrations. *Anal. Chem.* 92(8):6150–57
Lin MMJ, Prieve DC. 1983. Electromigration of latex induced by a salt gradient. *J. Colloid Interface Sci.* 95(2):327–39
Maass CC, Krüger C, Herminghaus S, Bahr C. 2016. Swimming droplets. *Annu. Rev. Condens. Matter Phys.* 7:171–93
Marbach S, Bocquet L. 2019. Osmosis, from molecular insights to large-scale applications. *Chem. Soc. Rev.* 48(11):3102–44
Marbach S, Yoshida H, Bocquet L. 2020. Local and global force balance for diffusiophoretic transport. *J. Fluid Mech.* 892:A6
Mauger C, Volk R, Machicoane N, Bourgoin M, Cottin-Bizonne C, et al. 2016. Diffusiophoresis at the macroscale. *Phys. Rev. Fluids* 1(3):034001
McCutcheon JR, McGinnis RL, Elimelech M. 2005. A novel ammonia–carbon dioxide forward (direct) osmosis desalination process. *Desalination* 174(1):1–11
McKenzie BE, Chu HCW, Garoff S, Tilton RD, Khair AS. 2022. Drop deformation during diffusiophoresis. *J. Fluid Mech.* 949:A17
Merkel TC, Bondar VI, Nagai K, Freeman BD, Pinnau I. 2000. Gas sorption, diffusion, and permeation in poly (dimethylsiloxane). *J. Polym. Sci. B Polym. Phys.* 38(3):415–34
Migacz RE, Ault JT. 2022. Diffusiophoresis in a Taylor-dispersing solute. *Phys. Rev. Fluids* 7(3):034202
Migacz RE, Durey G, Ault JT. 2023. Convection rolls and three-dimensional particle dynamics in merging solute streams. *Phys. Rev. Fluids* 8:114201
Möller FM, Kriegel F, Kieß M, Sojo V, Braun D. 2017. Steep pH gradients and directed colloid transport in a microfluidic alkaline hydrothermal pore. *Angew. Chem. Int. Ed.* 56(9):2340–44
Moran JL, Posner JD. 2017. Phoretic self-propulsion. *Annu. Rev. Fluid Mech.* 49:511–40
Palacci J, Abécassis B, Cottin-Bizonne C, Ybert C, Bocquet L. 2010. Colloidal motility and pattern formation under rectified diffusiophoresis. *Phys. Rev. Lett.* 104(13):138302
Park SW, Lee J, Yoon H, Shin S. 2021. Microfluidic investigation of salinity-induced oil recovery in porous media during chemical flooding. *Energy Fuels* 35(6):4885–92
Parry BR, Surovtsev IV, Cabeen MT, O'Hern CS, Dufresne ER, Jacobs-Wagner C. 2014. The bacterial cytoplasm has glass-like properties and is fluidized by metabolic activity. *Cell* 156(1):183–94
Paustian JS, Azevedo RN, Lundin STB, Gilkey MJ, Squires TM. 2013. Microfluidic microdialysis: spatiotemporal control over solution microenvironments using integrated hydrogel membrane microwindows. *Phys. Rev. X* 3(4):041010
Prieve DC, Anderson JL, Ebel JP, Lowell ME. 1984. Motion of a particle generated by chemical gradients. Part 2. Electrolytes. *J. Fluid Mech.* 148:247–69

Prieve DC, Malone SM, Khair AS, Stout RF, Kanj MY. 2019. Diffusiophoresis of charged colloidal particles in the limit of very high salinity. *PNAS* 116(37):18257–62
Prieve DC, Roman R. 1987. Diffusiophoresis of a rigid sphere through a viscous electrolyte solution. *J. Chem. Soc. Faraday Trans.* 83(8):1287–306
Provenzano PP, Inman DR, Eliceiri KW, Knittel JG, Yan L, et al. 2008. Collagen density promotes mammary tumor initiation and progression. *BMC Med.* 6(1):11
Raj RR, Shields CW, Gupta A. 2023. Two-dimensional diffusiophoretic colloidal banding: optimizing the spatial and temporal design of solute sinks and sources. *Soft Matter* 19(5):892–904
Ramírez-Hinestrosa S, Yoshida H, Bocquet L, Frenkel D. 2020. Studying polymer diffusiophoresis with non-equilibrium molecular dynamics. *J. Chem. Phys.* 152(16):164901
Ramm B, Goychuk A, Khmelinskaia A, Blumhardt P, Eto H, et al. 2021. A diffusiophoretic mechanism for ATP-driven transport without motor proteins. *Nat. Phys.* 17(7):850–58
Rasmussen MK, Pedersen JN, Marie R. 2020. Size and surface charge characterization of nanoparticles with a salt gradient. *Nat. Commun.* 11(1):2337
Raynal F, Bourgoin M, Cottin-Bizonne C, Ybert C, Volk R. 2018. Advection and diffusion in a chemically induced compressible flow. *J. Fluid Mech.* 847:228–43
Raynal F, Volk R. 2019. Diffusiophoresis, Batchelor scale and effective Péclet numbers. *J. Fluid Mech.* 876:818–29
Saad S, Natale G. 2019. Diffusiophoresis of active colloids in viscoelastic media. *Soft Matter* 15(48):9909–19
Sambamoorthy S, Chu HCW. 2023. Diffusiophoresis of a spherical particle in porous media. *Soft Matter* 19(6):1131–43
Schulz M, Smith RW, Sear RP, Brinkhuis R, Keddie JL. 2020. Diffusiophoresis-driven stratification of polymers in colloidal films. *ACS Macro Lett.* 9(9):1286–91
Sear RP. 2019. Diffusiophoresis in cells: a general nonequilibrium, nonmotor mechanism for the metabolism-dependent transport of particles in cells. *Phys. Rev. Lett.* 122(12):128101
Sear RP, Warren PB. 2017. Diffusiophoresis in nonadsorbing polymer solutions: the Asakura-Oosawa model and stratification in drying films. *Phys. Rev. E* 96(6):062602
Seo M, Park S, Lee D, Lee H, Kim SJ. 2020. Continuous and spontaneous nanoparticle separation by diffusiophoresis. *Lab Chip* 20(22):4118–27
Sheng JJ. 2014. Critical review of low-salinity waterflooding. *J. Petrol. Sci. Eng.* 120:216–24
Shi N, Abdel-Fattah A. 2021. Droplet migration into dead-end channels at high salinity enhanced by micelle gradients of a zwitterionic surfactant. *Phys. Rev. Fluids* 6(5):053103
Shi N, Nery-Azevedo R, Abdel-Fattah AI, Squires TM. 2016. Diffusiophoretic focusing of suspended colloids. *Phys. Rev. Lett.* 117(25):258001
Shim S. 2022. Diffusiophoresis, diffusioosmosis, and microfluidics: surface-flow-driven phenomena in the presence of flow. *Chem. Rev.* 122(7):6986–7009
Shim S, Nunes JK, Chen G, Stone HA. 2022. Diffusiophoresis in the presence of a pH gradient. *Phys. Rev. Fluids* 7(11):110513
Shimokusu TJ, Maybruck VG, Ault JT, Shin S. 2020. Colloid separation by CO_2-induced diffusiophoresis. *Langmuir* 36(25):7032–38
Shin S. 2020. Diffusiophoretic separation of colloids in microfluidic flows. *Phys. Fluids* 32(10):101302
Shin S. 2023. Directed colloidal assembly and banding via DC electrokinetics. *Biomicrofluidics* 17(3):031301
Shin S, Ault JT, Feng J, Warren PB, Stone HA. 2017a. Low-cost zeta potentiometry using solute gradients. *Adv. Mater.* 29(30):1701516
Shin S, Ault JT, Toda-Peters K, Shen AQ. 2020. Particle trapping in merging flow junctions by fluid-solute-colloid-boundary interactions. *Phys. Rev. Fluids* 5(2):024304
Shin S, Ault JT, Warren PB, Stone HA. 2017b. Accumulation of colloidal particles in flow junctions induced by fluid flow and diffusiophoresis. *Phys. Rev. X* 7(4):041038
Shin S, Doan VS, Feng J. 2019. Osmotic delivery and release of lipid-encapsulated molecules via sequential solution exchange. *Phys. Rev. Appl.* 12(2):024014
Shin S, Shardt O, Warren PB, Stone HA. 2017c. Membraneless water filtration using CO_2. *Nat. Commun.* 8(1):15181

Shin S, Um E, Sabass B, Ault JT, Rahimi M, et al. 2016. Size-dependent control of colloid transport via solute gradients in dead-end channels. *PNAS* 113(2):257–61

Shin S, Warren PB, Stone HA. 2018. Cleaning by surfactant gradients: particulate removal from porous materials and the significance of rinsing in laundry detergency. *Phys. Rev. Appl.* 9(3):034012

Shukla V, Volk R, Bourgoin M, Pumir A. 2017. Phoresis in turbulent flows. *New J. Phys.* 19(12):123030

Singh N, Vladisavljević GT, Nadal F, Cottin-Bizonne C, Pirat C, Bolognesi G. 2020. Reversible trapping of colloids in microgrooved channels via diffusiophoresis under steady-state solute gradients. *Phys. Rev. Lett.* 125(24):248002

Solomentsev Y, Anderson JL. 1994. Electrophoresis of slender particles. *J. Fluid Mech.* 279:197–215

Somasundar A, Qin B, Shim S, Bassler BL, Stone HA. 2023. Diffusiophoretic particle penetration into bacterial biofilms. *ACS Appl. Mater. Interfaces* 15(28):33263–72

Staffeld PO, Quinn JA. 1989. Diffusion-induced banding of colloid particles via diffusiophoresis: 2. Non-electrolytes. *J. Colloid Interface Sci.* 130(1):88–100

Stocker R. 2012. Marine microbes see a sea of gradients. *Science* 338(6107):628–33

Stout RF, Khair AS. 2014. A continuum approach to predicting electrophoretic mobility reversals. *J. Fluid Mech.* 752:R1

Stout RF, Khair AS. 2017. Influence of ion sterics on diffusiophoresis and electrophoresis in concentrated electrolytes. *Phys. Rev. Fluids* 2(1):014201

Tan H, Banerjee A, Shi N, Tang X, Abdel-Fattah A, Squires TM. 2021. A two-step strategy for delivering particles to targets hidden within microfabricated porous media. *Sci. Adv.* 7(33):eabh0638

Tang S, Zhang F, Gong H, Wei F, Zhuang J, et al. 2020. Enzyme-powered Janus platelet cell robots for active and targeted drug delivery. *Sci. Robot.* 5(43):eaba6137

Taylor GI. 1953. Dispersion of soluble matter in solvent flowing slowly through a tube. *Proc. R. Soc. A* 219(1137):186–203

Teng J, Rallabandi B, Ault JT. 2023. Diffusioosmotic dispersion of solute in a long narrow channel. *J. Fluid Mech.* 977:A5

Testa A, Dindo M, Rebane AA, Nasouri B, Style RW, et al. 2021. Sustained enzymatic activity and flow in crowded protein droplets. *Nat. Commun.* 12(1):6293

Tetteh JT, Brady PV, Ghahfarokhi RB. 2020. Review of low salinity waterflooding in carbonate rocks: mechanisms, investigation techniques, and future directions. *Adv. Colloid Interface Sci.* 284:102253

Tseng S, Su CY, Hsu JP. 2016. Diffusiophoresis of a charged, rigid sphere in a Carreau fluid. *J. Colloid Interface Sci.* 465:54–57

Velegol D, Garg A, Guha R, Kar A, Kumar M. 2016. Origins of concentration gradients for diffusiophoresis. *Soft Matter* 12(21):4686–703

Villermaux E. 2019. Mixing versus stirring. *Annu. Rev. Fluid Mech.* 51:245–73

Volk R, Bourgoin M, Bréhier CE, Raynal F. 2022. Phoresis in cellular flows: from enhanced dispersion to blockage. *J. Fluid Mech.* 948:A42

Wang K, Leville S, Behdani B, Batista CAS. 2022. Long-range transport and directed assembly of charged colloids under aperiodic electrodiffusiophoresis. *Soft Matter* 18(32):5949–59

Warmoeskerken MMCG, van der Vlist P, Moholkar VS, Nierstrasz VA. 2002. Laundry process intensification by ultrasound. *Colloids Surf. A* 210(2–3):277–85

Warren PB. 2020. Non-Faradaic electric currents in the Nernst-Planck equations and nonlocal diffusiophoresis of suspended colloids in crossed salt gradients. *Phys. Rev. Lett.* 124(24):248004

Williams I, Naderizadeh S, Sear RP, Keddie JL. 2022. Quantitative imaging and modeling of colloidal gelation in the coagulant dipping process. *J. Chem. Phys.* 156(21):214905

Williams I, Warren PB, Sear RP, Keddie JL. 2024. Colloidal diffusiophoresis in crossed electrolyte gradients: experimental demonstration of an "action-at-a-distance" effect predicted by the Nernst-Planck equations. *Phys. Rev. Fluids* 9(1):014201

Wilson JL, Shim S, Yu YE, Gupta A, Stone HA. 2020. Diffusiophoresis in multivalent electrolytes. *Langmuir* 36(25):7014–20

Xu J, Wang Z, Chu HCW. 2023. Unidirectional drying of a suspension of diffusiophoretic colloids under gravity. *RSC Adv*. 13(14):9247–59

Yang F, Rallabandi B, Stone HA. 2019. Autophoresis of two adsorbing/desorbing particles in an electrolyte solution. *J. Fluid Mech*. 865:440–59

Zydney AL. 1995. Boundary effects on the electrophoretic motion of a charged particle in a spherical cavity. *J. Colloid Interface Sci*. 169(2):476–85